DOI: 10.1002/ejic.201000257

New Approaches to 12-Coordination: Structural Consequences of Steric Stress, Lanthanoid Contraction and Hydrogen Bonding

Anthony S. R. Chesman,[a] David R. Turner,[a] Glen B. Deacon,[a] and Stuart R. Batten*[a]

Keywords: Lanthanides / Lanthanide contraction / Nitroso ligand / Hydrogen bonds / Steric hindrance

The anionic dinitrile ligand dicyanonitrosomethanide (dcnm), $C(CN)_2(NO)^-$, and the anion resulting from its addition product with water, carbamoylcyanonitrosomethanide (ccnm), $C(CN)(CONH_2)(NO)^-$, have been incorporated into lanthanoid complexes and display unusual η^2(N,O) nitroso coordination modes. $(Et_4N)_3[Ln(ccnm)_6]$ (**1Ln**; **1Ln** = **1La**, **1Ce**, **1Pr**, **1Nd**, **1Sm**) and $(Me_4N)_3[Ln(ccnm)_6]$ (**2Ln**; **2Ln** = **2La**, **2Ce**, **2Pr**, **2Nd**) are systems containing 12-coordinate homoleptic trianionic lanthanoidate complexes. The nitroso groups of the ccnm ligands form three-membered ring chelates with the lanthanoid metal centre, with the asymmetry of the nitroso η^2 interactions dependent upon the intramolecular N–H···O=N hydrogen bonding. Additional intermolecular hydrogen bonding interactions exist between adjacent amide and nitrile groups giving rise to 3D α-Po and 6,8-connected $(4^{12}.6^3)(4^{20}.6^8)$ networks in **1Ln** and **2Ln**, respectively. The compounds $(Me_4N)_3[Ln(dcnm)_6]$ (**3Ln**; **3Ln** = **3La**, **3Ce**, **3Nd**, **3Sm**) also contain a 12-coordinate trianionic lanthanoidate complex with the nitroso group exhibiting a highly symmetrical η^2 interaction. The sterically crowded environments of [Ln(18-crown-6)$(dcnm)_3$] (**4Ln**; **4Ln** = **4La**, **4Ce**, **4Pr**, **4Nd**) result in a shift towards a more asymmetric η^2 bonding of the nitroso group with decrease in the Ln^{3+} radius. There is a corresponding increase of the Ln–O–N angle, and one ligand is η^1(O) binding in **4Nd**. The dcnm ligands in the discrete complexes $[La(phen)_3(dcnm)_{(3-x)}Cl_x]$, $x \approx 0.25$ (**5**) (phen = 1,10-phenanthroline), $(Et_4N)[Ce(phen)_2(dcnm)_4]$ (**6a/b**, **6c**) and $[Ce(phen)_2(dcnm)Cl_2H_2O]$ (**7**) display a variety of coordination modes. Complex **5** has 1D chains formed by π–π stacking of adjacent phen co-ligands. Complexes **6** contain the monoanionic complex $[Ce(phen)_2(dcnm)_4]^-$ with two geometric isomers present in the crystal structure of **6a/b**. Complex **7** forms extended 1D chains via hydrogen bonding between coordinated water and chloride atoms and an extensive array of face-to-face π interactions.

Introduction

The dicyanonitrosomethanide ligand (dcnm), $C(CN)_2(NO)^-$, offers two distinct functional groups which may coordinate to metals; two nitrile arms and a nitroso group. This anionic ligand has been used in a number of transition metal complexes, typically displaying either η^1(O) or η^1(N) bonding (depending upon the hardness of the metal), with a few examples of η^2(N,O) coordination known.[1] The dcnm ligand readily undergoes nucleophilic addition of a protic solvent, such as water or methanol, across a single nitrile arm, e.g. the addition of water to form carbamoylcyanonitrosomethanide (ccnm).[2] Such addition reactions have previously only been observed to occur in the presence of a transition metal yielding complexes containing the anionic products.[3] Nucleophilic addition may also be catalysed by an acid, but this approach results in protonation of the nitroso group, yielding a neutral ligand with fewer modes of coordination available.[4]

The unique chemistry of lanthanoids offers access to a diverse array of coordination modes[5] but this is coupled with significant synthetic challenges owing to the unpredictability of complex formation.[6] These difficulties need to be overcome if the novel magnetic[7] and luminescent[8] properties of these metals are to be harnessed. In addition, the lanthanoid contraction can be responsible for a pronounced change in the structure of complexes that contain the same ligating species, e.g. $LnCp_3$ complexes.[9a] Conversely, in certain ligand systems the effect of the lanthanoid contraction may not be significant enough to cause structural changes across the entire series.[9b]

The chemistry of *homoleptic* 12-coordinate lanthanoids is heavily dominated by the $[Ln(NO_3)_6]$ moiety[5a,10] although other examples incorporating bi-,[11] tri-,[12,13] and hexadentate[14,15] ligands have been documented. The η^2(N,O) coordination by the dcnm ligand with three-membered chelate rings offered an alternative and new approach to highly coordinated homoleptic complexes.[16]

We have communicated the novel η^2(N,O) symmetrical binding mode of dcnm in a series of homoleptic 12-coordinate lanthanoid complexes $(Et_4N)_3[Ln(dcnm)_6]$ (Ln = La, Ce, Nd and Gd).[16] Previously dcnm has only been seen to coordinate in a very asymmetric fashion to lanthanoids in

[a] School of Chemistry, Monash University,
Clayton, VIC 3800, Australia
Fax: +61-3-9905-4606
E-mail: stuart.batten@sci.monash.edu.au

Supporting information for this article is available on the WWW under http://dx.doi.org/10.1002/ejic.201000257.

the complexes $[Nd(dcnm)_3(hmpa)_4]$[1d] and $[Yb(dcnm)_2(hmpa)_4][dcnm]$[1e] (hmpa = hexamethylphosphoramide). Bonding of the nitroso groups in these complexes displays a significant degree of distortion with differences in Ln–O and Ln–N bond lengths in the range of 0.30–0.64 Å. This asymmetry is presumably due to the hmpa ligands sterically crowding the coordination sphere of the lanthanoid. The only previous example of the dcnm anion with near symmetrical η^2(N,O) bonding is the 3D network of $[Ba(dcnm)_2(H_2O)]$ [(Ba–N)–(Ba–O) = 0.026(6) Å].[1g]

There are few examples of complexes with η^2(N,O) binding of a nitroso group to lanthanoids. In $[(TMPO)_3Sm]_2$ (TMPO = 2,2,6,6-tetramethylpiperidinyl 1-oxide), which contains two μ-η^2:η^1 bridging nitroso groups and four η^1(O) terminal ligands,[17] the η^2 Sm–O and Sm–N bond lengths of the ligand are 2.36 and 2.54 Å, respectively (a difference of 0.18 Å). A more symmetric η^2 bonding mode is seen in the complex $[GdCp_2(acet)]_2$ (acet = acetoneoximate), where two μ-η^2:η^1 nitroso groups bridge the gadolinium atoms with η^2 Gd–O and Gd–N bond lengths of 2.38 and 2.40 Å, respectively.[18a] Other examples of N–O groups binding in a η^2 fashion to lanthanoids to form three-membered rings are known, such as the hydroxylaminato ligands in $K[M(ONiPr_2)_4]$[18b] and $[Cp_2MON(CH_2C_6H_5)_2]_2$ (M = Y, Sm).[18c] The NO groups again adopt a μ-η^2:η^1 bonding mode with significant asymmetry observed in the bond lengths of the three-membered ring.

Herein we report the formation of 12-coordinate lanthanoidate trianions using the dcnm and ccnm ligands. The latter allows for strong intra- and intermolecular hydrogen bonding that affects the η^2(N,O) coordination mode. We further report coordination of the neutral co-ligands 18-crown-6 and 1,10-phenanthroline in lanthanoid/dcnm complexes and the effects that the consequential steric crowding has on the η^2 bonding mode of the nitroso group of the dcnm ligand. The changes in both coordination number and bonding mode are contrasted within comparable systems.

Results and Discussion

Although the nucleophilic addition of protic solvents to dcnm normally requires the presence of a transition metal the water addition anion species $C(CN)(CONH_2)(NO)^-$ (ccnm) can be obtained as synthetically useful Na^+, Ag^+ or R_4N^+ salts directly from malononitrile (Scheme 1). It is likely that dcnm anions are intermediates, as we have also observed the addition of water to Na(dcnm) to form Na(ccnm) under reflux conditions without a transition metal being present.

Thus a previous synthetic methodology for Ag(dcnm)[1c] was altered to yield Ag(ccnm) in a one pot reaction without isolation of a dcnm derivative (Scheme 1). This synthetic approach then permits the synthesis of standard solutions of tetraalkylammonium salts of the ligand through metathesis (Scheme 1, step III) and the subsequent synthesis of rare-earth complexes containing ccnm. The use of different

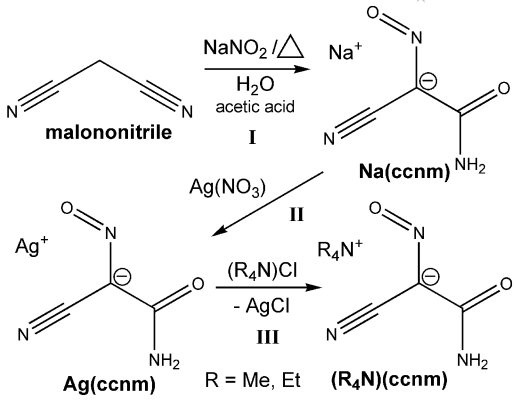

Scheme 1. Addition of water across one of the nitrile arms of Na(dcnm), yielding Na(ccnm) and the exchange of the silver counter cation with a tetraalkylammonium cation.

tetraalkylammonium salts of the ligand allows for examination of the effects the counter cations may play upon crystal packing and consequent complex configurations.

Reaction of tetraalkylammonium salts of ccnm, (R_4N)(ccnm) where R = Et and Me, with hydrated lanthanoid chlorides in methanol (followed in some cases by vapour diffusion of diethyl ether) yields crystals of the complexes $(Et_4N)_3[Ln(ccnm)_6]$ (**1Ln**; **1Ln** = **1La**, **1Ce**, **1Pr**, **1Nd**, **1Sm**) and $(Me_4N)_3[Ln(ccnm)_6]$ (**2Ln**; **2Ln** = **2La**, **2Ce**, **2Pr**, **2Nd**), respectively (Scheme 2). Crystals of the complex **1Sm** were isolated through an alternative methodology adapted from the one-pot synthesis of complexes of the type $(Et_4N)_3[Ln(dcnm)_6]$.[16]

$$6\,(R_4N)(ccnm) + LnCl_3{\cdot}xH_2O \rightarrow (R_4N)_3[Ln(ccnm)_6] + 3\,(R_4N)Cl + x\,H_2O$$

R = Et, **1Ln** = **1La**, **1Ce**, **1Pr**, **1Nd**, **1Sm**; R = Me, **2Ln** = **2La**, **2Ce**, **2Pr**, **2Nd**

$$6\,Ag(ccnm) + 3\,(Et_4N)Br + SmCl_3{\cdot}6H_2O \rightarrow (Et_4N)_3[Sm(ccnm)_6] + 3\,AgCl + 3\,AgBr + 6\,H_2O$$

Scheme 2. Reaction of tetraalkylammonium salts of ccnm with lanthanoid chlorides.

The trianionic complex $[Ln(ccnm)_6]^{3-}$ contains six anionic ligands adopting an approximately octahedral geometry around the lanthanoid metal centre. Similar geometry has been observed in $(Et_4N)_3[Ln(dcnm)_6]$ complexes.[16] The crystal structures are of lower symmetry than their dcnm counterparts ($Ia\bar{3}$), with the isomorphous **1Ln** complexes crystallising in the space group $P2_1/n$ and **2La** and **2Pr**–**2Nd** crystallising in $C2/c$ and $C2$, respectively. The structure of **1Ln** contains one complete $[Ln(ccnm)_6]^{3-}$ complex and its three associated cations (with one present over two half occupancy positions) in the asymmetric unit. The structure of **2Ln** also contains a complete formula unit, $(Me_4N)_3[Ln(ccnm)_6]$, in the asymmetric unit but consists of two halves of two crystallographically unique anionic complexes. Both structures therefore contain six unique η^2(N,O) interactions. Despite the $[Ln(ccnm)_6]^{3-}$ complexes being isocompositional in **1Ln** and **2Ln** there are some significant differences in the coordination modes of the ccnm ligands in the two structural series.

The six unique η^2 bonding modes of the nitroso groups in **1Ln** vary in their degree of asymmetry although in all cases the Ln–O distance is the shorter of the two interactions, (Figure 1, Table 1). Within the cerium complex **1Ce**, for example, the difference between the bond lengths of Ce–N and Ce–O for the six unique ccnm ligands lies in the range 0.078(6)–0.284(6) Å. This range of values is representative of the rest of the anionic complexes in the **1Ln** series (Figure 2). The (Ln–N)–(Ln–O) differences may be related to the lanthanoid contraction since the average Δ values [0.14 (La), 0.15 (Ce), 0.15 (Pr), 0.16 (Nd), 0.18 (Sm)] increase with the decrease of ionic radii across the lanthanoid series. The nature of the η^2 interactions is most likely attributable to the degree of intramolecular hydrogen bonding within the complexes, rather than from a steric influence of the ccnm ligand. The amide containing carbamoyldicyanomethanide anion, $C(CN)_2(CONH_2)^-$ is known to form strong hydrogen bonding motifs with both the amide and nitrile functionalities.[19] In **1Ln** each ccnm amide group is orientated towards the nitroso group of a neighbouring ligand (Figure 1). However, the ligands are not all equivalent with four nitroso groups accepting one hydrogen bond, one nitroso group accepting two hydrogen bonds and one nitroso group not participating in any hydrogen bonding at all. The steric crowding around the centre of the anion prohibits the nitroso groups from participating in any *inter*molecular bonding.

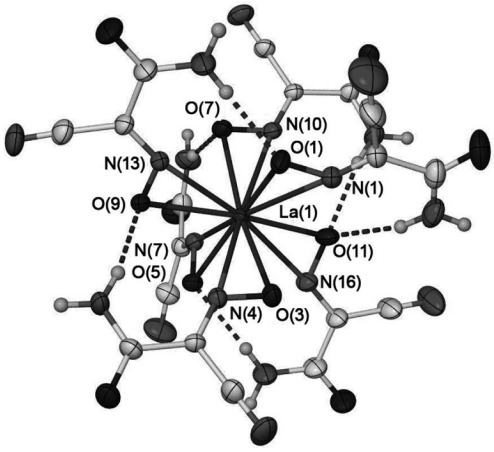

Figure 1. The discrete $[La(ccnm)_6]^{3-}$ complex, representative of the **1Ln** series, has a pseudo-octahedral geometry and displays intramolecular hydrogen bonding between hydrogen atoms of the amide group and the oxygen atoms of neighbouring nitroso groups (ellipsoids displayed at 30% probability).

Table 1. Bond lengths [Å] and angles [°] of nitroso bonding to the lanthanoid in **1Ln**.

	L1 O1/N1	**L2** O3/N4	**L3** O5/N7	**L4** O7/N10	**L5** O9/N13	**L6** O11/N16
La–N	2.786(3)	2.649(3)	2.680(3)	2.700(3)	2.649(3)	2.750(4)
La–O	2.529(3)	2.512(2)	2.601(2)	2.544(2)	2.575(2)	2.589(3)
Δ[a]	0.257(6)	0.137(5)	0.079(5)	0.156(5)	0.074(5)	0.161(7)
La–O–N	86.8(2)	81.0(2)	78.8(2)	82.0(2)	78.5(2)	82.7(2)
Ce–N	2.748(3)	2.600(4)	2.612(3)	2.647(3)	2.617(3)	2.734(4)
Ce–O	2.464(3)	2.483(3)	2.534(3)	2.515(3)	2.527(3)	2.537(3)
Δ[a]	0.284(6)	0.117(7)	0.078(6)	0.132(6)	0.090(6)	0.197(7)
Ce–O–N	87.7(2)	80.0(2)	78.6(2)	80.9(2)	79.1(2)	84.2(2)
Pr–N	2.740(3)	2.584(3)	2.596(3)	2.641(3)	2.609(2)	2.729(3)
Pr–O	2.444(2)	2.471(2)	2.524(2)	2.505(2)	2.511(2)	2.518(2)
Δ[a]	0.296(5)	0.113(5)	0.072(5)	0.136(5)	0.098(4)	0.211(5)
Pr–O–N	88.1(2)	79.8(1)	78.2(1)	81.0(1)	79.4(1)	84.8(2)
Nd–N	2.747(3)	2.564(3)	2.580(3)	2.624(3)	2.587(3)	2.724(3)
Nd–O	2.429(2)	2.455(2)	2.507(2)	2.484(2)	2.495(2)	2.504(2)
Δ[a]	0.318(5)	0.109(5)	0.073(5)	0.140(5)	0.092(5)	0.220(5)
Nd–O–N	89.3(2)	79.6(2)	78.2(2)	81.1(2)	79.1(2)	85.3(2)
Sm–N	2.791(3)	2.545(2)	2.550(3)	2.604(2)	2.559(2)	2.721(3)
Sm–O	2.402(2)	2.430(2)	2.477(2)	2.452(2)	2.452(2)	2.472(2)
Δ[a]	0.389(5)	0.115(4)	0.073(5)	0.152(4)	0.107(4)	0.249(5)
Sm–O–N	92.7(2)	79.8(1)	78.1(2)	81.4(2)	79.4(1)	86.4(2)

[a] Δ = (Ln–N) – (Ln–O).

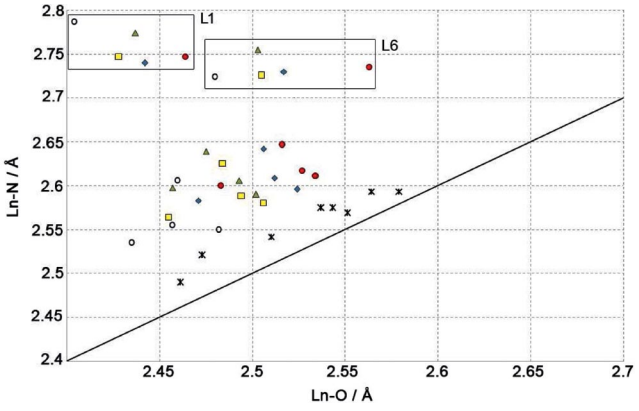

Figure 2. Plot of Ln–O vs. Ln–N bond lengths in the complexes **1La** (triangles), **1Ce** (circles), **1Pr** (diamonds), **1Nd** (squares) and **1Sm** (hollow circle). The data points for the two ligands (L1 and L6) with the most distorted η^2 interactions are highlighted by the boxes. Data obtained from the more symmetrical $(Et_4N)_3[Ln(dcnm)_6]$ structures (Ln = La, Ce, Nd, Gd) is contrasted as crosses.[16] The line represents a perfectly symmetrical binding mode.

A closer examination of the intramolecular hydrogen bonding can be used to rationalise the observed differences in the Ln–O and Ln–N distances. Figure 2, a plot of Ln–O vs. Ln–N for all nitroso groups in the **1Ln** series, shows that there are two η^2 interactions in each structure that are significantly more distorted that the remaining four. These ligands contain Ln–N distances greater than 2.7 Å. One of these two ligands (L1, containing O1/N1) acts as a hydrogen-bond acceptor for the shortest hydrogen bond in the complex which is also one of the most directional in terms of the H···O–N angle, apparently strong enough to distort the bonding mode of the ligand. The second most distorted η^2 bonding mode belongs to L6 (O11/N16), which receives two hydrogen bonds (one of which also has a relatively obtuse approach angle), effectively pivoting the ligand around the oxygen atom and elongating the Ln–N bond.

Such phenomena are not unknown, with a previous report showing that hydrogen bonding is able to affect H_2O–M bonds in transition metal complexes.[20] The remaining

intramolecular hydrogen bonding occurs at more acute H···O–N angles. Representative intramolecular hydrogen bonding distances for **1La** is shown in Table S1.

Only six of the twelve amide hydrogen atoms are involved in intramolecular hydrogen bonding with the remaining six directed away from the complex and participating in *inter*molecular interactions. Each $[Ln(ccnm)_6]^{3-}$ complex in **1Ln** hydrogen bonds to six others, via a variety of different synthons, to give an overall distorted α-Po network with the counter cations residing in the square windows of the network (Figure 3). Intermolecular interactions include the R_2^2 (8) amide synthon,[21] single NH···nitrile interactions and NH interactions between adjacent complexes that incorporate three ccnm ligands with both a nitrile and an amide oxygen atom acting as acceptor groups.

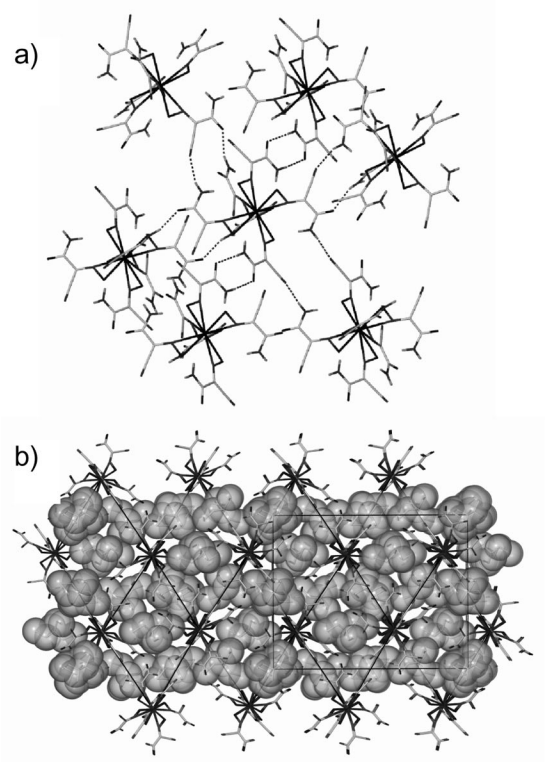

Figure 3. (a) Various hydrogen bonding motifs between discrete complexes in **1Ln**, forming (b) an overall distorted α-Po network with Et_4N^+ cations in the square windows of the network (viewed along *a*-axis), cations shown with van der Waals spheres.

The identity of the $(Me_4N)_3[Ln(ccnm)_6]$ complexes are clearly established by the X-ray crystal structures of **2La**, **2Pr** and **2Nd**, though due to the effects of disorder and twinning, the refinements of the last two are of sufficient quality only to unambiously determine the connectivity. However the nature and extent of associated solvent of crystallisation presents problems. For **2La**, the crystal structure is optimised with one methanol and half a molecule of water per complex, and the less reliable praseodymium and neodymium crystal structures have two thirds of a methanol per complex. The infrared spectra of freshly prepared samples are very similar and no significant changes are observed with time, especially in the complex ν(OH)/ν(NH) region (see Exp. Sect.). On the other hand elemental and thermogravimetric analyses suggest that **2La** has two methanol molecules rather than one methanol and half a water molecule, and that **2Pr** has one methanol and one water molecule per complex. Elemental analyses for **2Ce** (amorphous) and **2Nd** best fit for two water molecules per complex but a solvation of one methanol and one water molecule per complex is also plausible (see Exp. Sect.). The lanthanum complex is not isomorphous with **2Pr** and **2Nd**, consistant with a solvation difference, and suggesting the similarity of the infrared spectra is perhaps misleading as a guide to solvation. Despite the uncertainty over the solvent of crystallisation, however, the presence of the 12-coordinate $[Ln(ccnm)_6]^{3-}$ complex ions cannot be disputed.

The structure of **2Ln** is markedly different from that of **1Ln** both in terms of the bonding within the $[Ln(ccnm)_6]^{3-}$ complex and the *inter*molecular interactions. The changes are presumably brought about by the use of a different counter-cation, allowing a change in the intermolecular interactions which have a "knock-on" effect on the coordination geometry. The smaller cation also results in cavities in the lattice which contain solvent, an observation supported by microanalyses and contrasting unsolvated **1Ln**.

The ligands in **2La** display more symmetrical bonding modes than those in **1Ln**, with an average difference between Ln–N and Ln–O bond lengths of 0.12 Å The structure of **2La** contains two distinct pseudo-octahedral metal complexes (half of each is crystallographically unique) with different coordination environments and hydrogen bonding (Figure 4). One of the molecules contains opposing ligands that are co-planar with each other with adjacent ligands around the complex in mutually perpendicular orienations (Figure 4, a) whereas the other molecule has a less ordered coordination sphere (Figure 4, b). All of the ccnm ligands display a slight deviation from a symmetrical η^2(N,O) binding mode (Table 2). For example, the difference between the bond lengths of La–$N_{nitroso}$ and La–$O_{nitroso}$ lie in the range 0.057(7)–0.152(7) Å for **2La** (Table 2).

The intramolecular hydrogen bonding within **2Ln** is more uniform than that observed in **1Ln** with each nitroso group accepting a hydrogen bond from one other ccnm ligand. The environment around the molecule containing La(2) (see Figure 4, a) is the most uniform with similar hydrogen bonding distances and angles for all interactions (Table S2). The hydrogen bonding between adjacent ligands occurs at H···O–N angles nearing 90°, a reflection of the pseudo-octahedral arrangement of the planar ligands. The high symmetry is also reflected by the similarity of the bond lengths of the nitroso group coordination (Table 3). Intramolecular hydrogen bonding of the molecule containing La(1) is complicated by the fact that the species also accepts hydrogen bonds from lattice methanol molecules. While two of the unique interactions are similar to those observed in the La(2) molecule, one hydrogen bond is significantly different, with a more linear H···O=N angle akin to those observed in **1Ln**. Unlike the **1Ln** complexes, where more linear interactions distort the η^2 ligation, the acceptor ligand of

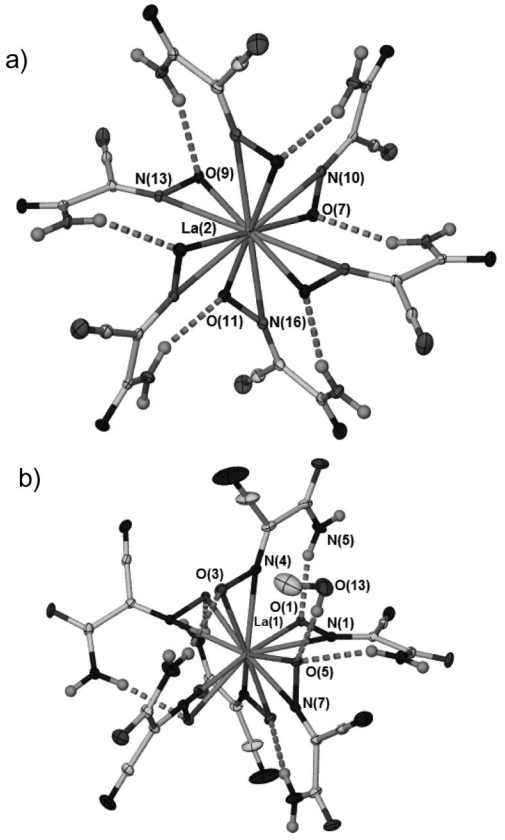

Figure 4. The coordination environments of the two crystallographically unique $[La(ccnm)_6]^{3-}$ anions in the structure of $(Me_4N)_3[La(ccnm)_6]$ (**2La**) with a) the symmetrical anion with mutually perpendicular ligands and b) the less symmetrical anion which has interactions with lattice methanol. Ellipsoids displayed at 30% probability, only symmetry unique positions labelled for clarity.

Table 2. Bond lengths [Å] and angles [°] of nitroso bonding to the lanthanoid in **2La**. The L4–L6 values for the ccnm ligands of the more symmetrical $[La(ccnm)_6]^{3-}$ anion.

	L1 O1/N1	L2 O3/N4	L3 O5/N7	L4 O7/N10	L5 O9/N13	L6 O11/N16
La–N	2.646(4)	2.613(4)	2.671(4)	2.661(4)	2.651(3)	2.665(4)
La–O	2.494(3)	2.556(3)	2.533(3)	2.543(4)	2.531(3)	2.540(3)
Δ[a]	0.152(7)	0.057(7)	0.138(7)	0.118(8)	0.120(6)	0.125(7)
La–O–N	81.6(2)	77.7(2)	81.2(2)	80.3(2)	80.5(2)	80.7(2)

[a] Δ = (La–N) – (La–O).

the most linear hydrogen bond in **2La** has the most symmetrical coordination. The interaction is, however, significantly longer than others in this study (i.e. the H-bonding donor···acceptor distance is longer by approximately 0.2 Å, Table S2) which presumably reduces the effect that the hydrogen bonding can exert on the η^2 binding mode.

The crystal packing in **2La** is also different to that of **1Ln**, with all of the ccnm ligands involved in NH···O hydrogen bonding to adjacent $[Ln(ccnm)_6]^{3-}$ complexes but no NH···nitrile interactions (Figure 5). The hydrogen bonding network is more complicated than this initial description implies, with one molecule acting as an 8-connecting node (La1) and the other as a 6-connecting node (La2). Adjacent

Table 3. Selected bond lengths [Å] and angles [°] for $(Me_4N)_3[Ln(dcnm)_6]$ (**3Ln**).

	3La	3Ce	3Nd	3Sm
Ln(1)–N(1)	2.600(2)	2.578(4)	2.538(3)	2.525(4)
Ln(1)–O(1)	2.580(2)	2.542(3)	2.519(2)	2.473(3)
Δ[a]	0.020(4)	0.036(7)	0.019(5)	0.052(7)
Ln(1)–O(1)–N(1)	76.32(14)	76.8(2)	75.94(16)	77.4(2)

[a] Δ = (Ln–N) – (Ln–O).

molecules are joined in one of two ways; a single NH···O hydrogen bond (involving one ligand from each complex) or by two NH···O hydrogen bonds (involving a total of four ligands). The La(1) complex is connected to eight others by four "double" hydrogen bond interactions and four single interactions (Figure 5, a). The 6-connecting molecule forms hydrogen bonds in a roughly octahedral geometry with two NH···O interactions between adjacent species in all cases (Figure 5, b). Overall a 3D 6,8-connected network with $(4^{12}.6^3)(4^{20}.6^8)$ topology is formed, with the counter cations occupying the spaces within framework (Figure S1).

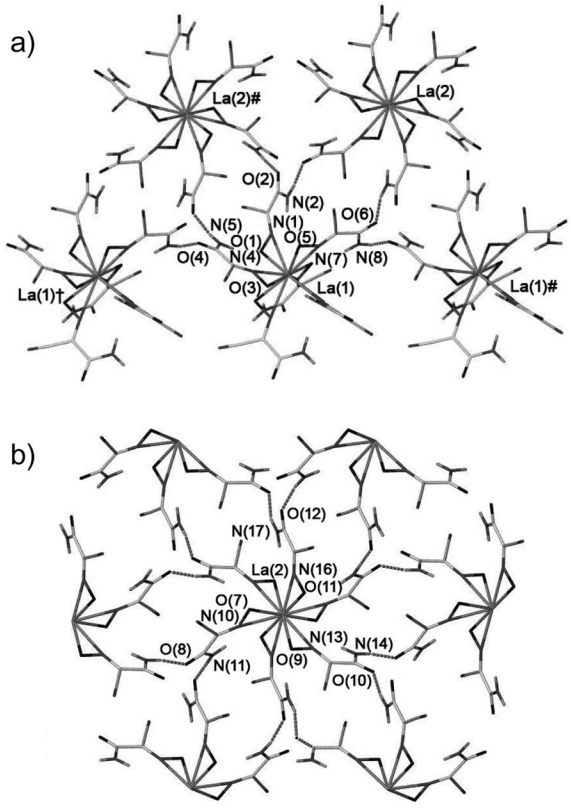

Figure 5. Intermolecular hydrogen bonding of **2La** (a) the 8-connecting La(1) molecule (only the symmetry unique half of the hydrogen bonding around the molecule is shown for clarity) and (b) the 6-connecting La(2) complex. Symmetry elements used: † = 1/2 + *x*, 1/2 + *y*, *z*; ‡ = 1 – *x*, 2 – *y*, –*z*; # = *x* – 1/2, *y* – 1/2, *z*.

The lower symmetry structures of **2Pr** and **2Nd** contain significant disorder, resulting in them only being useful for determining the local connectivity of the individual complexes, with the asymmetric unit containing one and a half unique anions. The whole unique anion has three of the six

ccnm ligands disordered over two positions. One configuration of the ligands forms a symmetrical coordination environment around the lanthanoid atom, as seen around La(2) in **2La**, while the other configuration is less symmetrical, similar to that of La(1).

The marked differences in the crystal structures of **1Ln** and **2Ln** associated with the change from Et_4N^+ to Me_4N^+ counter cations encouraged us to investigate $(Me_4N)_3[Ln(dcnm)_6]$ complexes to compare with our reported $(Et_4N)_3[Ln(dcnm)_6]$ (Ln = La, Ce, Nd, Gd) derivatives.[16] The complexes $(Me_4N)_3[Ln(dcnm)_6]$ (**3Ln**; **3Ln** = **3La**, **3Ce**, **3Nd**, **3Sm**) were crystallised by diffusion of diethyl ether into a methanolic solution of tetramethylammonium dicyanonitrosomethanide and the corresponding hydrated rare-earth chloride salt. Initially the complexes were synthesised by allowing the methanolic solution to evaporate to dryness but this required the manual removal of the $(Me_4N)Cl$ co-product, and did not allow for the effective isolation of the pure product. Attempted synthesis through either method with rare-earth nitrate salts resulted only in the formation of hexanitratolanthanoidate complexes.[10b,22] Interestingly, the gadolinium analogue of **3Ln** did not appear to be accessible through the vapour diffusion method. After isolation from the reaction solution and exposure to the atmosphere for one year the infrared spectra of **3La** and **3Nd** develop an extra weak peak at 1662 and 1661 cm^{-1}, respectively. This peak may be attributable to a carbonyl group, as seen in the spectra of $[Ln(ccnm)_6]^{3-}$ complexes, as the reactive nitrile group of the dcnm ligand undergoes nucleophilic addition of atmospheric water to form a carbamoyl group.

The $[Ln(dcnm)_6]^{3-}$ anions in **3Ln** (Figure 6) are analogous to those previously reported for the tetraethylammonium analogues.[16] The dcnm anions bind to the metal through the nitroso group, exhibiting a highly symmetrical η^2(N,O) bonding mode in all cases (Table 3). When measured from the midpoint of the nitroso group the six ligands are arranged in an octahedral geometry around the central lanthanoid. These structures demonstrate that the $[Ln(dcnm)_6]^{3-}$ anions are a stable, reproducible species with the configuration of the molecule independent of the counter cations present.

Complexes **3La**, **3Ce** and **3Nd** are isomorphous, crystallising in the rhombohedral space group $R\bar{3}$, and contain three complex ions per unit cell. The smaller lanthanoid containing complex **3Sm** crystallises in $P6_3/m$ with only two complexes per unit cell. The asymmetric units of both structural types contain one unique coordinating dcnm ligand and one sixth of a lanthanoid metal centre which resides on a threefold inversion axis. The complexes $(Et_4N)_3[Ln(dcnm)_6]$, which crystallise in the cubic space group $Ia\bar{3}$, also contain one sixth of the complex in the asymmetric unit.[16]

The Ln–N and Ln–O distances within the complexes **3Ln** follow a trend across the series, with a gradual shortening of the bonds resulting from the lanthanoid contraction (Table 3). The contraction also results in an increase of the Ln–O–N angle as the ligand–metal distance is reduced. The

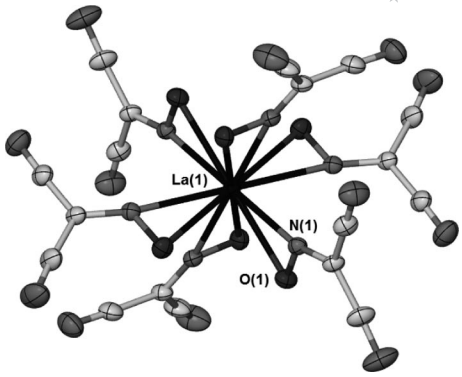

Figure 6. The discrete $[La(dcnm)_6]^{3-}$ anion within the crystal structure of $(Me_4N)_3[La(dcnm)_6]$, **3La**, lies on a threefold inversion centre (ellipsoids shown at 50% probability). The anions within the structures of **3Ce**, **3Nd** and **3Sm** have the same pseudo-octahedral coordination geometry.

nitroso groups have symmetrical η^2 bonding modes, with the differences in the Ln–O and Ln–N bonds considerably smaller than those observed for **1Ln** and **2Ln**. In all cases the Ln–O bond is marginally shorter, reflecting the oxophilic nature of the rare-earth metals.

The crystal structures of **3La**, **3Ce**, and **3Nd** consist of layers of $2(Me_4N)^+\cdot[Ln(dcnm)_6]^{3-}$ in the *ab* plane with substantial gaps between these layers (Figure S2). As a result, the crystal packing reveals significant regions of disorder within the lattice. The third counter-cation is disordered within the lattice and required an isotropic refinement. The structure of **3Sm** has a similar layered structure to the other compounds, however the third counter cation was able to be located and satisfactorily refined, in the spaces between the $2(Me_4N)^+\cdot[Ln(dcnm)_6]^{3-}$ sheets (Figure 7). It is evident that there are also large pores and highly disordered solvent present between the layers. Elemental analysis indicates the solvent consists of one molecule each of methanol and water per two $[La(dcnm)_6]^{3-}$ anions in **3La**, and one and a half molecules of water and one molecule of methanol per two $[Ln(dcnm)_6]^{3-}$ anions in **3Ce**, **3Nd**, and **3Sm**.

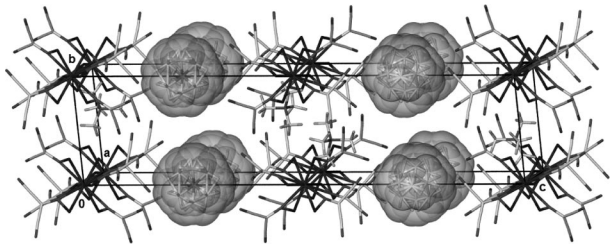

Figure 7. The structure of **3Sm** showing the remaining counter cation disordered between these layers.

When considering the difficulties in determining the solvation of complexes **2Ln** and **3Ln**, in comparison to **1La** and $(Et_4N)_3[Ln(dcnm)_6]$,[16] it is apparent the counter-cation plays a significant role in the crystal packing and the formation of cavities in which lattice solvent may reside. In this series of complexes it is evident that the size of the

tetraethylammonium counter-cation may be complementary to those of the $[Ln(ccnm/dcnm)_6]^{3-}$ complexes allowing for more efficient packing.

The neutral co-ligands 18-crown-6 and 1,10-phenanthroline were incorporated into complexes to examine whether the symmetry of the bonding of the nitroso group could be influenced through the introduction of ligands that would crowd the coordination sphere of the metal, as observed earlier in the complexes $[Nd(dcnm)_3(hmpa)_4]$ and $[Yb(dcnm)_2(hmpa)_4](dcnm)$.[1d,1e]

Compounds of the type [Ln(18-crown-6)(dcnm)$_3$] (**4Ln**; **4Ln** = **4La**, **4Ce**, **4Pr**, **4Nd**) were synthesised from the reaction of $(Me_4N)(dcnm)$ with the corresponding lanthanoid chloride in the presence of one equivalent of 18-crown-6 (Scheme 3).

$$LnCl_3{\cdot}xH_2O + 18\text{-crown-6} + 3\ (Me_4N)(dcnm) \rightarrow [Ln(18\text{-crown-6})(dcnm)_3] + 3\ (Me_4N)Cl + x\ H_2O$$

Scheme 3. Synthesis of [Ln(18-crown-6)(dcnm)$_3$] (**4Ln**).

The complexes **4La**–**4Pr** are isomorphous, whereas there is a substantial change in structure with the smaller rare-earth in **4Nd**. In the isomorphous complexes **4La**–**4Pr** the 12-coordinate lanthanoid atom resides near the centre of the crown ether, with the six Ln–O interactions from the crown ether having bond lengths in the range 2.671(4)–2.773(4) Å for **4La**, 2.663(2)–2.770(2) Å for **4Ce** and 2.659(2)–2.762(2) Å for **4Pr** (Figure 8). The lanthanoid coordination sphere is completed by three dcnm ligands with two on one side of the crown and one on the other. The lone dcnm ligand displays the same highly symmetrical η^2 chelation that is observed in the complexes **3Ln**. The 18-crown-6 ring is slightly puckered towards the single ligand allowing space to accommodate two ligands on the opposite side of the metal. Within this more sterically crowded environment the ligands display less symmetric binding modes.

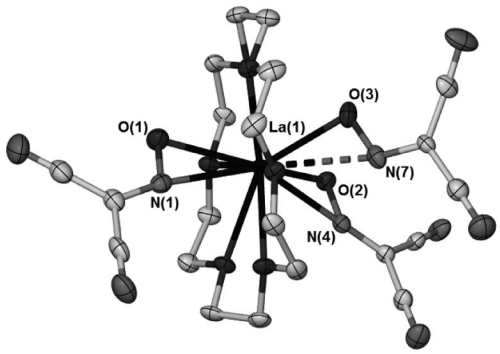

Figure 8. Structure of [La(18-crown-6)(dcnm)$_3$] (**4La**). Ellipsoids shown at 50% probability, hydrogen atoms are omitted for clarity. Compounds **4Ce** and **4Pr** are isomorphous. The dashed line represents an elongated Ln–N interaction.

In the lanthanum complex **4La** one of these sterically crowded dcnm ligands has a La–O vs. La–N bond length difference of 0.124(9) Å, which is similar to the asymmetry of the bonding of the ligands in **2Ln** (Table 2). The adjacent ligand exhibits highly stressed η^2 bonding with a shortened La–O bond length of 2.478(4) Å and an elongated La–N distance of 2.896(5) Å. The degree of asymmetry of this ligation is further evidenced by the larger corresponding Ln–O–N angle of 94.7(3)° (Table 4). The effect of steric crowding is even more pronounced with **4Ce** and **4Pr**, with the difference in Ln–O and Ln–N bond lengths of the most aymmetric ligand (O3/N7) increasing as the ionic radius of the metal ion decreases. The increase in asymmetry is also reflected in the corresponding Ln–O–N angles which increase across the series (Table 4). The contraction of the 4*f* metals across the series gives less space for the ligands to bind and hence they adopt more asymmetric bonding modes.

Table 4. Selected bond lengths [Å] and angles [°] for complexes [Ln(18-crown-6)(dcnm)$_3$] (**4Ln**).

	4La	**4Ce**	**4Pr**	**4Nd**
	O(1)/N(1)			
Ln–N	2.591(6)	2.563(2)	2.541(2)	2.627(2)
Ln–O	2.540(5)	2.510(2)	2.469(2)	2.445(2)
Δ[a]	0.051(11)	0.053(4)	0.072(4)	0.182(4)
Ln–O–N	77.7(3)	77.7(1)	78.2(1)	83.1(1)
	O(2)/N(4)			
Ln–N	2.646(5)	2.619(2)	2.601(2)	2.650(2)
Ln–O	2.522(4)	2.498(2)	2.480(1)	2.395(2)
Δ[a]	0.124(9)	0.121(4)	0.121(3)	0.255(4)
Ln–O–N	80.8(3)	80.5(1)	80.5(1)	86.1(1)
	O(3)/N(7)			
Ln···N	2.896(5)	2.926(2)	2.980(2)	3.342(2)
Ln–O	2.478(4)	2.450(2)	2.433(2)	2.379(2)
Δ[a]	0.418(9)	0.476(4)	0.547(4)	0.963(4)
Ln–O–N	94.7(3)	97.7(1)	101.5(1)	128.3(1)

[a] Δ = (Ln–N) – (Ln–O).

The lanthanoid contraction manifests itself more sharply at neodymium with a distinct structural change, as **4Nd** crystallises in the space group $P\bar{1}$ in contrast to the other complexes (*Pbca*). **4Nd** shows an even more sterically crowded environment with the crown ether significantly curved out of plane (Figure 9). The curvature is due to a distortion that accommodates the reduced size of the central lanthanoid atom. The lanthanoid contraction also results in a shortening of the Nd–O interactions between the metal centre and crown ether to a range of 2.546(2)–2.704(2) Å, a larger distance range than observed with **4La**–**4Pr**, and a markedly lower limit. None of the bonding dcnm ligands demonstrate a symmetric η^2 bonding mode, with the least asymmetric having a difference between Ln–O and Ln–N bond lengths of 0.182(4) Å. The ligand which bonds through O(3) and N(7) in **4La**–**4Pr** is bonding solely through the oxygen atom in **4Nd** with the Nd–N(7) distance being 3.342(3) Å, far too long to be considered an interaction, and with a difference between Ln–O and Ln–N bond lengths of 0.963(4) Å.

The change in the coordination environment between **4Pr** and **4Nd** has similarities to that in the series of nitrate analogues.[23] The compounds [Ln(18-crown-6)$(NO_3)_3$] (Ln = La, Ce, Pr, Nd) contain a 12 coordinate lanthanoid atom

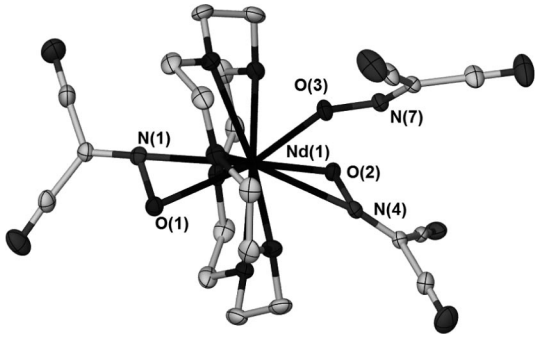

Figure 9. The complex [Nd(18-crown-6)(dcnm)$_3$] (**4Nd**). Ellipsoids shown at 50% probability, hydrogen atoms omitted for clarity.

complexed by a hexadentate 18-crown-6. They are similar to **4La**–**4Pr**, with two nitrate anions on one side of the crown ether and one on the other. Smaller nitratolanthanoid complexes with 18-crown-6 have the composition [La(18-crown-6)$(NO_3)_2$](NO_3) (Ln = Nd, Eu, Gd).[24] The lanthanoid is coordinated in these complexes by only two nitrate anions, one on either side of the crown ether. This change in the series of 18-crown-6 complexes with nitrate resembles the current observation of a transition between **4Pr** and **4Nd**, although the nitrate analogues show neodymium can exist in both forms. As nitrate gives a four-membered chelate ring compared with a three-membered ring for dcnm, steric hindrance near the metal is less for the latter, hence the change of coordination numbers is from 12 to 11 for dcnm but 12 to 10 for nitrate.

IR spectroscopy demonstrated a peak shift for ν_{as}(C–N=O) in the complexes **4Ln**. Thus, **4La**–**4Pr** have two close peaks near 1420 cm^{-1} which are due to the different η^2 bonding modes whereas **4Nd** shows a larger separation of the corresponding bands due to both η^2 and η^1 bonding modes being present. This is also evidenced by the two peaks at approximately 1188 cm^{-1} and 1186 cm^{-1} which for **4La**–**4Pr** correspond to ν_s(C–N=O) while there are three peaks in this region for **4Nd**. In comparison the complexes **3Ln** and $(Et_4N)_3$[Ln(dcnm)$_6$] have only one peak at 1412 cm^{-1} which can be attributable to ν_{as}(C–N=O) and one at 1200 cm^{-1}, attributable to ν_s(C–N=O), reflecting the η^2 bonding only in these higher symmetry complexes. With all the aforementioned complexes the IR spectra show minimal shifts in the peaks corresponding to the nitrile groups, probably due to the fact that they do not coordinate to the metal centre in these complexes.

The use of 1,10-phenanthroline (phen) as a co-ligand resulted in four very different complexes with a variety of coordination environments. The mixed system [La(phen)$_3$(dcnm)$_{3-x}$Cl$_x$], $x \approx 0.25$ (**5**) crystallised on diffusion of diethyl ether vapour into a methanolic solution of (Et_4N)(dcnm) and lanthanum chloride in the presence of *two* equivalents of 1,10-phenanthroline (Figure 10, a). One 10-coordinate complex exists in the asymmetric unit with a disordered η^1-dcnm/chloride ligand site (approximately 3:1). The *three* phenanthroline co-ligands chelate to the lanthanum in a uniform fashion [La–N bonds in the range 2.715(5)–2.800(5) Å]. The dcnm ligands have mixed coordination modes with two ligands (including the disordered position) displaying η^1(O) bonding and one having an asymmetric η^2(N,O) bonding of the nitroso group (Table 5). Even with the largest lanthanoid ion, crowding by the phen ligands obviates the possibility of 12 coordination. The packing of the complexes in the structure of **5** displays significant face-to-face interactions between the 1,10-phenanthroline co-ligands forming 1D π-stacked chains parallel to the *c*-axis (Figure 10, b).[25]

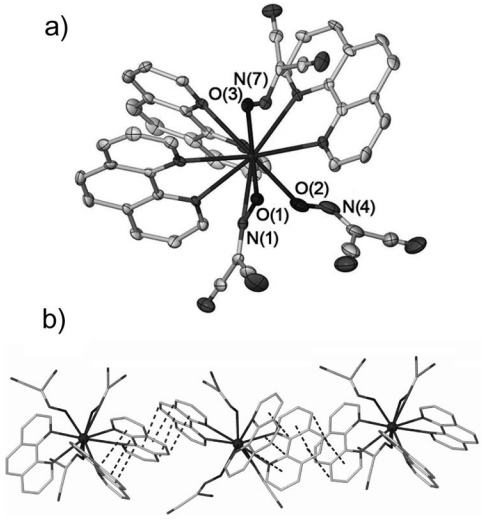

Figure 10. (a) The structure of [La(phen)$_3$(dcnm)$_3$] (**5**) containing two η^1(O) bonding dcnm ligands and one η^2(N,O) ligand. Ellipsoids shown at 50% probability, hydrogen atoms omitted for clarity. The O(2) ligand has a 3/4 occupancy with 1/4 chloride in the same site (not shown for clarity). (b) The complexes pack via an array of π–π interactions (C···ring centroid interactions shown).

Table 5. Selected bond lengths [Å] and angles [°] for [La(1,10-phen)$_3$(dcnm)$_3$] **5**.

	O(1)/N(1)	O(2)/N(4)	O(3)/N(7)
La–N	2.641(5)	3.56[b]	3.39[b]
La–O	2.536(4)	2.501(9)	2.436(4)
Δ[a]	0.105(9)	1.059	0.954
La–O–N	80.0(3)	141.9	127.5(3)

[a] Δ = (La–N) – (La–O). [b] Non-bonding length.

A search of the CSD[26] revealed complex **5** to be unusual with few previously reported lanthanoid compounds containing three chelating 1,10-phenanthroline ligands. Complexes of the type [Ln(phen)$_3$(NCS)$_3$] (Ln = Pr, Nd)[27] contain a nine-coordinate lanthanoid with the ligands arranged pseudo-octahedrally if the 1,10-phenanthroline ligands are viewed as occupying only one averaged coordination site. There are no nitrate analogues comparable to the [La(phen)$_3$(dcnm)$_3$] complex with the only known nitrato phenanthroline lanthanoid complexes being of the form [Ln(phen)$_2$(NO$_3$)$_3$] (Ln = La, Ce, Pr, Nd, Sm, Eu, Gd, Dy, Tb, Er, Lu),[28] in which the lanthanoid atom is 10 coordinate.

When a reaction solution containing (Et_4N)(dcnm), 1,10-phenanthroline and cerium chloride hydrate was evaporated to dryness it yielded (Et_4N)[Ce(phen)$_2$(dcnm)$_4$] in two iso-

compositional forms. In the first reaction the resulting crystal structure contained two geometric isomers of $[Ce(phen)_2(dcnm)_4]^-$ (**6a/b**) (Figure 11), with subsequent syntheses yielding a crystal structure containing only one unique *transoid* metal complex (**6c**). Geometric isomers in lanthanoid coordination chemistry are rare but not unknown,[29] and previously the repeated synthesis of a specific geometric isomer has proven to be problematic.[29d] The complex **6a/b** crystallises in the space group *C*2/*c* with the asymmetric unit containing one and a half $[Ce(phen)_2(dcnm)_4]^-$ complexes and one and a half Et_4N^+ countercations. Both $[Ce(phen)_2(dcnm)_4]^-$ complexes are 10-coordinate and contain four dcnm ligands, two of which display η^2(N,O) coordination of the nitroso group while the remaining two ligands coordinate in an η^1 fashion through the oxygen atom. The remaining coordination sites are occupied by two chelating 1,10-phenanthroline ligands.

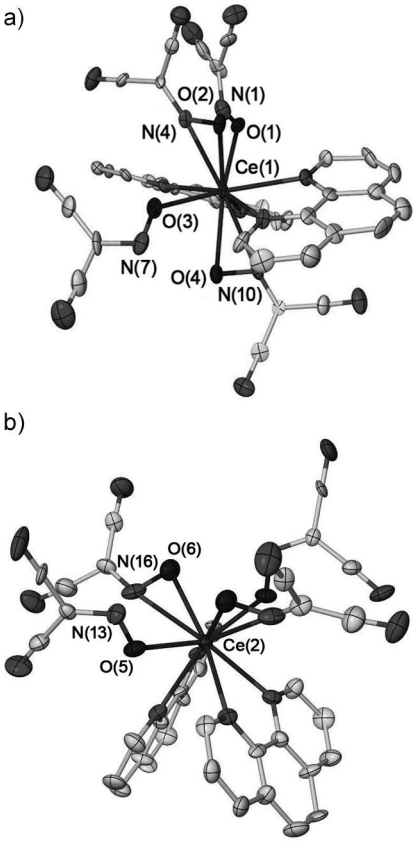

Figure 11. The two unique $[Ce(phen)_2(dcnm)_4]^-$ complexes in the structure of **6a/b** (a) *transoid* (**6a**) and (b) *cisoid* (**6b**) phenanthroline ligands. Ellipsoids displayed at 50% probability, hydrogen atoms omitted for clarity. Only the symmetry unique part of the Ce(2) complex is labelled (the other half is related by the operator $1 - x$, y, $1/2 - z$).

The most pronounced sign of difference between the two complexes is the relative positions of the phenanthroline ligands, namely *transoid* in one complex, that containing Ce(1) (**6a**), and *cisoid* in the other (**6b**) (Figure 11, parts a and b, respectively). The change in the coordination sphere appears to bring about a change in the degree of asymmetry in the η^2(N,O) bonding mode, with that in the *cisoid* complex being significantly more distorted than those in the *transoid* complex (Table 6). The η^2 interactions in the *transoid* complex have a difference between Ce–O and Ce–N bond lengths in a similar range to those observed in the $[Ln(dcnm)_6]^{3-}$ complexes, whereas the distortion in the *cisoid* complex is greater than that caused by the intramolecular hydrogen bonding in the $[Ln(ccnm)_6]^{3-}$ species. It can be rationalised that steric crowding occurs due to the *cisoid* conformation that forces the dcnm ligand away from a symmetric bonding mode. The two η^2 dcnm ligands in the *transoid* complex are bound to opposite sides of the cerium atom (150° apart using N–O centroids) whereas those in the *cisoid* complex are significantly closer (109°). In fact, all four dcnm ligands within the *cisoid* complex are bound in the same hemisphere of the metal, leading to a significant degree of crowding. In contrast, those of the *transoid* complex are almost arranged in pseudo-octahedral equatorial positions with the phenanthroline groups occupying the apical positions, thereby achieving the maximum separation between ligands. The η^1(O) ligands in the two complexes do not differ significantly in their bonding lengths (Table 6). In all cases the Ce–O bond lengths of these ligands are marginally longer than those in the η^2 ligands and the Ce···N non-bonding distance is approximately 3.4 Å.

Table 6. Selected bond lengths [Å] and angles [°] for the $[Ce(1,10\text{-phen})_2(dcnm)_4]^-$ anions in $(Et_4N)[Ce(1,10\text{-phen})_2(dcnm)_4]$ (**6a/b**). Ligands containing O(1), O(2), O(3) and O(4) from **6a**, remainder from **6b**.

	Ce–O	Ce–N	Δ[a]	Ce–O–N
O(1)/N(1)	2.458(9)	3.496(13)[b]	1.038(22)	134.6(7)
O(2)/N(4)	2.542(8)	2.591(10)	0.049(18)	77.6(6)
O(3)/N(7)	2.477(9)	3.472(13)[b]	0.995(22)	132.3(7)
O(4)/N(10)	2.483(8)	2.624(10)	0.141(18)	81.4(6)
O(5)/N(13)	2.413(9)	3.335(11)[b]	0.922(20)	124.7(7)
O(6)/N(16)	2.459(10)	2.824(12)	0.365(22)	92.1(8)

[a] Δ = (Ce–N) – (Ce–O). [b] Non-bonding length.

The crystal packing in **6a/b** is interesting with the two different anionic complexes packing in sheets with their own kind (Figure S3). Both sheets contain π–π interactions between the molecules, but there is little interaction between these layers. The tetraethylammonium cations are in the layer containing the *cisoid* complexes, positioned such that they are surrounded almost exclusively by nitrile groups.

Repeated attempts to remake crystals of **6a/b** using the same synthetic method yielded only crystals containing the single geometric isomer **6c**. In **6c** the complex crystallises in the space group $P\bar{1}$ with only a *transoid* form of the metal complex present, with three dcnm ligands displaying a η^2(N,O) coordination mode, with the remainder η^1(O) giving overall 11-coordination, cf. **6a/b** (Table 7). The η^1 and one η^2 coordinating ligands are disordered over two positions, pivoting around the nitroso bond and consequently not affecting the degree of symmetry in bonding between the two positions. Crystal packing is dominated by π–π interactions between the complexes to form 1D chains (Figure S4), with the tetraethylammonium counter-cation residing within the lattice.

Table 7. Selected bond lengths [Å] and angles [°] for the $[Ce(1,10\text{-phen})_2(dcnm)_4]^-$ anions in $(Et_4N)[Ce(1,10\text{-phen})_2(dcnm)_4]$ (**6c**).

	Ce–O	Ce–N	Δ[a]	Ce–O–N
O(1)/N(1)	2.487(3)	2.702(4)[b]	0.215(7)	85.0(2)
O(2)/N(4)	2.503(3)	2.632(4)	0.129(7)	81.0(2)
O(3)/N(7)	2.521(4)	2.656(5)[b]	0.135(9)	81.5(2)
O(4)/N(10)	2.473(4)	3.348(4)	0.875(7)	122.8(3)

[a] Δ = (Ce–N) – (Ce–O). [b] Non-bonding length.

The complex $[Ce(phen)_2(dcnm)Cl_2(H_2O)]$ (**7**) was synthesised by vapour diffusion of diethyl ether into the reaction solution, rather than total evaporation as in the case of **6a/b**, yielding several crystals of **7** after one week. The nine-coordinate complex contains two *transoid* 1,10-phenanthroline ligands, with Ce–N bonds lying in the range 2.647(2)–2.713(2) Å, two terminal chlorides, one η^2 dcnm and a water ligand (Figure 12, a). The two *cis* chloride ligands bond to the cerium in an almost perpendicular fashion (Cl–Ce–Cl = 82.52(2)°). The dcnm ligand displays a slightly asymmetric η^2 bonding mode with a bond difference between Ce–N and Ce–O of 0.097(4) Å. Although there are two bulky co-ligands coordinated to the cerium the dcnm ligand is quite removed from them. Indeed, if the η^2 ligand and phenanthroline ligands are viewed as monodentate then the complex can be described as having a distorted octahedral geometry with the mutually *trans* phenanthroline ligands not interfering with the dcnm coordination mode. The water ligand forms hydrogen bonds in which the two chloride ligands on an adjacent complex act as the hydrogen-bond acceptors,[30] with O···Cl distances of 3.084(2) and 3.111(2) Å and O–H···Cl angles of 164(3) and 154(3)°, respectively. These intermolecular interactions are responsible for the formation of 1D chains that propagate parallel to the crystallographic *a*-axis. Both of the 1,10-phenanthroline ligands interdigitate with those on neighbouring chains in two directions giving an extensive array of face-to-face π-interactions (Figure 12, b). The interplanar phen···phen distances are 3.34 and 3.33 Å in one direction and 3.19 and 3.32 Å in the other, well inside the sum of the van der Waals radii for two aromatic rings.

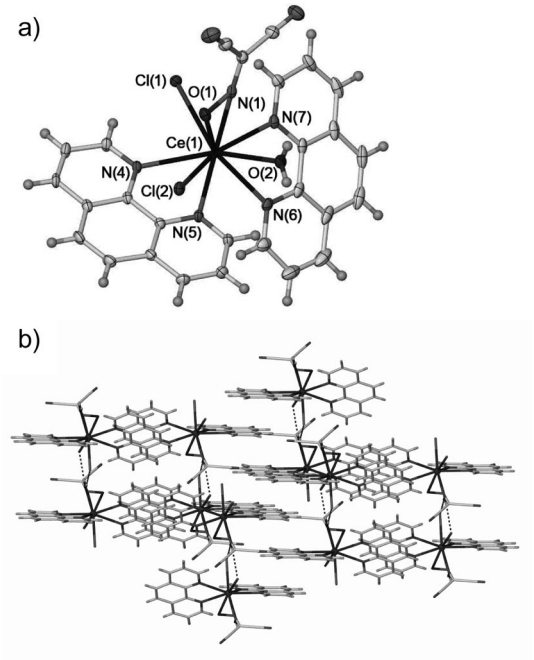

Figure 12. (a) The discrete complex $[Ce(phen)_2(dcnm)Cl_2(H_2O)]$ (**7**). Selected bond lengths [Å] and angles [°]: Ce(1)–O(1), 2.490(2); Ce(1)–N(1), 2.587(2); Ce(1)–Cl(1), 2.857(1); Ce(1)–Cl(2), 2.828(1); Ce(1)–O(2), 2.534(2); O(1)–Ce(1)–N(1), 29.64(5); Ce(1)–O(1)–N(1), 79.29(10). Ellipsoids displayed at 50% probability. (b) Hydrogen bonded 1D chains in the structure of **7** pack via face-to-face π-stacking in two directions between 1,10-phenanthroline co-ligands.

Conclusions

Several new series of rare-earth complexes containing the carbamoylcyanonitrosomethanide or dicyanonitrosomethanide ligands have been synthesised and structurally characterised. Use of the ligands provides a new approach to twelve and other high coordination lanthanoid complexes, involving three-membered rings in contrast to the four-membered rings of nitrato complexes that have hitherto dominated 12-coordinate lanthanoid complexes. These new complexes display variously distorted η^2(N,O) binding modes of the nitroso group, from the highly symmetrical interactions within $[Ln(dcnm)_6]^{3-}$ anions to η^1 bonds due to steric constraints and/or the size of the rare-earth element used in complexes incorporating 18-crown-6 and 1,10-phenanthroline.

Experimental Section

General: All materials and solvents were purchased from standard commercial sources and used without further purification. No protective atmosphere was required. Ag(dcnm)[1c] and Ag(ccnm)[31] were prepared by literature methods. Tetraalkylammonium (R = Me, Et) salts of the ligands were synthesised by a metathesis reaction (Scheme 1) and used as a standard solution. Infrared data were collected using a Perkin–Elmer ATR-FTIR spectrometer. Elemental analyses were performed by the Campbell Microanalytical Laboratory of the University of Otago, New Zealand. TGA was conducted on a Perkin–Elmer Pyris1 instrument under a N_2 atmosphere at a heating rate of 10 °C/min.

Synthesis of $(Et_4N)_3[Ln(ccnm)_6]$ (1Ln): $(Et_4N)(ccnm)$ (132 mg, 589 μmol) dissolved in methanol (1 mL) was added to solutions of the respective $LnCl_3{\cdot}xH_2O$ (88 μmol, La/$CeCl_3{\cdot}7H_2O$, 33 mg, Pr/Nd/$Sm_3{\cdot}6H_2O$, 32 mg) in methanol (1 mL). Needle crystals formed within three days. **1La**, 29 mg, 27%; m.p. 220–224 °C. IR (ATR): $\tilde{\nu}$ = 3386 (m), 3296 (m), 3240 (m), 3180 (m), 2993 (w), 2219 (m), 1663 (s), 1603 (m), 1458 (m), 1394 (m), 1203 (m), 1121 (m), 998 (w), 783 (w), 674 cm^{-1} (w). $C_{42}H_{72}LaN_{21}O_{12}$ (1202.06): calcd. C 41.97, H 6.04, N 24.47; found C 41.81, H 6.00, N 24.23. **1Ce**, 17 mg, 6%; m.p. 217–218 °C. IR (ATR): $\tilde{\nu}$ = 3387 (sh), 3294 (m), 3241 (m), 3178 (m), 2220 (w), 1654 (s), 1600 (m), 1485 (w), 1414 (s), 1198 (m), 1115 (s), 951 (w), 674 cm^{-1} (w). $C_{42}CeH_{72}N_{21}O_{12}$ (1203.27): calcd. C 41.92, H 6.03, N 24.45; found C 41.86, H 5.92, N 24.40. **1Pr**, 21 mg. 20%; m.p. 214–216 °C. IR (ATR): $\tilde{\nu}$ = 3388 (m), 3296 (m), 3242 (m), 3181 (m), 2219 (w), 1655 (s), 1600 (m), 1483 (w), 1457 (m), 1412 (m), 1201 (m), 1119 (m), 999 (w), 950 (w),

674 cm^{-1} (w). $C_{42}H_{72}N_{21}O_{12}Pr$ (1204.06): calcd. C 41.90, H 6.03, N 24.43; found C 41.87, H 6.09, N 24.63. **1Nd**, 25 mg, 24%; m.p. 213-215 °C. IR (ATR): $\tilde{\nu}$ = 3386 (m), 3297 (m), 3246 (m), 3180 (m), 3034 (vw), 2991 (vw), 2227 (m), 1664 (m), 1604 (w), 1484 (m), 1456 (w), 1409 (s), 1267 (w), 1200 (vs), 1122 (m), 1031 (vw), 1000 (w), 949 (w), 673 cm^{-1} (w). $C_{42}H_{72}N_{21}NdO_{12}$ (1207.40): calcd. C 41.78, H 6.01, N 24.36; found C 41.98, H 6.20, N 24.65.

Synthesis of $(Et_4N)_3[Sm(ccnm)_6]$ (1Sm): An excess of Ag(ccnm) (500 mg, 2476 μmol) was added to $(Et_4N)Br$ (238 mg, 1134 μmol) and $SmCl_3{\cdot}6H_2O$ (138 mg, 378 μmol) in methanol (10 mL). The solution was stirred covered from light for two hours and filtered to remove the AgBr/Cl precipitate and excess Ag(ccnm). The volume of the reaction solution was reduced to 2 mL under reduced pressure. A diffusion of diethyl ether into the reaction solution resulted in crystallisation of the product. The product was washed with methanol to dissolve $(Et_4N)_2(ccnm)_2{\cdot}H_2O$ which co-crystallised, resulting in the dissolution of some of the product (78 mg, 17%); m.p. 205–207 °C. IR (ATR): $\tilde{\nu}$ = 3383 (m), 3295 (m), 3246 (m), 3177 (m), 2993 (w), 2217 (m), 1662 (s), 1603 (m), 1456 (m), 1394 (m), 1202 (m), 1172 (vw), 1120 (m), 998 (w), 783 (w), 672 cm^{-1} (w). $C_{42}H_{72}N_{21}O_{12}Sm$ (1213.52): calcd. C 41.57, H 5.98, N 24.24; found C 41.32, H 6.12, N 24.37. An attempted synthesis from preformed $(Et_4N)(ccnm)$ was unsuccessful.

Synthesis of $(Me_4N)_3[Ln(ccnm)_6]$ (2Ln): A solution of $(Me_4N)(ccnm)$ (100 mg, 537 μmol) in methanol (1 mL) was added to solutions of the respective $LnCl_3{\cdot}xH_2O$ (89 μmol, La/$CeCl_3{\cdot}7H_2O$, 33 mg, Pr/$NdCl_3{\cdot}6H_2O$, 32 mg) in methanol (1 mL). Needle crystals formed within three days. **2La·2MeOH**, 35 mg, 36%; m.p. 201–203 °C. IR (ATR): $\tilde{\nu}$ = 3396 (m), 3300 (m), 3241 (m), 3183 (m), 3042 (vw), 2220 (w), 1678 (sh), 1651 (s), 1599 (m), 1484 (m), 1458 (m), 1411 (m), 1286 (vw), 1199 (m), 1116 (s), 949 (w), 673 cm^{-1} (w); thermogravimetric analysis: calcd. weight loss lattice solvent removal, 5.84%; observed weight loss, 5.88%. $C_{32}H_{56}LaN_{21}O_{14}$ (1097.83): calcd. C 35.01, H 5.14, N 26.70; found C 34.61, H 5.10, N 26.47. **2Ce·2H$_2$O**, 43 mg, 45%; m.p.198–200 °C. IR (ATR): $\tilde{\nu}$ = 3395 (m), 3298 (m), 3245 (m), 3182 (m), 3039 (vw), 2219 (w), 1678 (sh), 1657 (s), 1601 (m), 1484 (m), 1458 (m), 1412 (m), 1199 (m), 1118 (m), 949 (w), 674 cm^{-1} (w). $CeC_{30}H_{52}N_{21}O_{14}$ (1070.98): calcd. C 33.64, H 4.89, N 27.46; found C 33.22, H 4.69, N 27.24. **2Pr·H$_2$O·MeOH**, 36 mg, 38%; m.p. 199–201 °C. IR (ATR): $\tilde{\nu}$ = 3393 (m), 3296 (m), 3241 (m), 3180 (m), 3041 (vw), 2219 (w), 1678 (sh), 1653 (s), 1598 (m), 1484 (m), 1459 (m), 1411 (m), 1200 (m), 1116 (m), 949 (w), 673 cm^{-1} (w); thermogravimetric analysis: calcd. weight loss lattice solvent removal, 4.61%; observed weight loss, 4.86%. $C_{31}H_{54}N_{21}O_{14}Pr$ (1085.80): calcd. C 34.29, H 5.01, N 27.09; found C 34.02, H 4.93, N 27.50. **2Nd·2H$_2$O**, 20 mg, 21%; m.p. 200–202 °C. IR (ATR): $\tilde{\nu}$ = 3394 (m), 3297 (m), 3243 (m), 3179 (m), 3041 (vw), 2221 (w), 1678 (sh), 1654 (s), 1601 (m), 1483 (m), 1459 (w), 1411 (s), 1270 (w), 1200 (s), 1118 (s), 949 (w), 673 cm^{-1} (w). $C_{30}H_{52}N_{21}NdO_{14}$ (1075.10): calcd. C 33.51, H 4.88, N 27.36; found C 33.26, H 4.68, N 27.28.

Synthesis of $(Me_4N)_3[Ln(dcnm)_6]$ (3Ln): $(Me_4N)(dcnm)$ (70 mg, 416 μmol) was dissolved in methanol (1 mL) and added to solutions of the respective $LnCl_3{\cdot}xH_2O$ (69 μmol; La/$CeCl_3{\cdot}7H_2O$, 26 mg, Nd/$SmCl_3{\cdot}6H_2O$, 25 mg) dissolved in methanol (1 mL). The reaction vial was placed in larger vial containing diethyl ether (4 mL) and sealed allowing for vapour diffusion. Hexagonal crystals formed within 3 d, identified by X-ray crystallography as **3Ln**. Elemental analysis and representative thermogravimetric measurements indicate the degree of solvation. **3La·H$_2$O·0.5MeOH**, 47 mg, 72%; m.p. 172–175 °C. IR (ATR): $\tilde{\nu}$ = 3219 (br), 3034 (w), 2231 (s), 2213 (sh), 1485 (m), 1416 (m), 1301 (sh), 1269 (w), 1241 (w), 1198 (s), 950 cm^{-1} (m); thermogravimetric analysis: calcd. weight loss lattice solvent removal, 3.54%; observed weight loss, 4.02%. $C_{30.5}H_{40}La_1N_{21}O_{7.5}$ (959.69): calcd. C 38.17, H 4.20, N 30.65; found C 38.41, H 4.11, N 31.11. **3Ce·0.75H$_2$O·0.5MeOH**, 14 mg, 21%; m.p. 170–173 °C. IR (ATR): $\tilde{\nu}$ = 3208 (br), 3034 (w), 2231 (w), 2213 (sh), 1485 (m), 1415 (m), 1302 (sh), 1267 (w), 1242 (w), 1197 (s), 950 cm^{-1} (m). $C_{30.5}H_{39.5}Ce_1N_{21}O_{7.25}$ (956.39): calcd. C 38.30, H 4.16, N 30.76; found C 38.33, H 4.10, N 31.13. **3Nd·0.75H$_2$O·0.5MeOH**, 42 mg, 64%; m.p. 168–170 °C. IR (ATR): $\tilde{\nu}$ = 3185 (br), 3035 (w), 2230 (s), 2209 (sh), 1485 (m), 1413 (m), 1302 (w), 1268 (m), 1241 (w), 1200 (s), 949 cm^{-1} (m); thermogravimetric analysis: calcd. weight loss lattice solvent removal, 3.08%; observed weight loss, 3.35%. $C_{30.5}H_{39.5}N_{21}Nd_1O_{7.25}$ (960.52): calcd. C 38.13, H 4.15, N 30.62; found C 38.18, H 4.23, N 31.15. **3Sm·0.75H$_2$O·0.5MeOH**, 43 mg, 65%; m.p. 149–151 °C, IR (ATR): $\tilde{\nu}$ = 3496 (vw/br), 3035 (vw), 2981 (vw), 2875 (vw), 2229 (m), 1485 (m), 1411 (m), 1268 (m), 1200 (s), 949 cm^{-1} (m). $C_{30.5}H_{39.5}N_{21}O_{7.25}Sm_1$ (966.64): calcd. C 37.90, H 4.12, N 30.43; found C 38.04, H 4.04, N 30.35.

Synthesis of [Ln(18-crown-6)(dcnm)$_3$] (4Ln): $(Me_4N)(dcnm)$ (50 mg, 297 μmol) was dissolved in methanol (1 mL) and added to solutions of the respective $LnCl_3{\cdot}xH_2O$ (105 μmol; La/$CeCl_3{\cdot}7H_2O$, 38 mg, Pr/$NdCl_3{\cdot}6H_2O$, 37 mg) dissolved in methanol (1 mL). 18-crown-6 (28 mg, 105 μmol) dissolved in water (1 mL) was added to the reaction solution which was allowed to slowly evaporate. Tabular needles formed over 5 d, identified by X-ray crystallography as **4Ln**. **4La**, 31 mg, 45%; m.p. 235–240 °C. IR (ATR): $\tilde{\nu}$ = 2948 (m), 2980 (w), 2227 (s), 1472 (w), 1420 (s), 1354 (m), 1291 (w), 1260 (m), 1188 (s), 1082 (vs), 969 (s), 838 cm^{-1} (m). $C_{21}H_{24}LaN_9O_9$ (685.38): calcd. C 36.78, H 3.53, N 18.40; found C 36.98, H 3.55, N 18.44. **4Ce**, 26 mg, 39%; m.p. 232–235 °C. IR (ATR): $\tilde{\nu}$ = 2948 (m), 2890 (w), 2227 (m), 1471 (w), 1422 (s), 1354 (m), 1291 (w), 1259 (m), 1186 (s), 1074 (vs), 968 (s), 838 cm^{-1} (m). $C_{21}H_{24}CeN_9O_9$ (686.08): calcd. C 36.73, H 3.53, N 18.37; found C 37.12, H 3.63, N 18.37. **4Pr**, 22 mg, 32%. IR (ATR): $\tilde{\nu}$ = 3181 (vw), 2225 (w), 1655 (m), 1601 (w), 1485 (w), 1462 (w), 1422 (m), 1198 (m), 1173 (m), 1107 (w), 1075 (s), 1059 (sh), 951 (s), 880 (w), 837 cm^{-1} (m). $C_{21}H_{24}N_9O_9Pr$ (687.08): calcd. C 36.68, H 3.52, N 18.34; found C 36.52, H 3.72, N 18.27. **4Nd**, 20 mg, 30%; m.p. 228–232 °C. IR (ATR): $\tilde{\nu}$ = 2940 (m), 2883 (w), 2226 (s), 1457 (w), 1424 (m), 1394 (m), 1359 (w), 1296 (w), 1251 (w), 1176 (s), 1076 (vs), 960 (s), 838 cm^{-1} (m). $C_{21}H_{24}N_9NdO_9$ (688.08): calcd. C 36.62, H 3.52, N 18.31; found C 36.79, H 3.71, N 18.78.

Synthesis of $[La(phen)_3(dcnm)_{2.75}Cl_{0.25}]$ (5): 1,10-Phenanthroline (47 mg, 237 μmol) and $LaCl_3{\cdot}7H_2O$ (44 mg, 118 μmol) were dissolved in methanol (1 mL). A solution of $(Et_4N)(dcnm)$ (80 mg, 357 μmol) in methanol (1 mL) was added resulting in a light white precipitate. Water (500 μmol) was added causing the precipitate to dissolve. The reaction vial was then placed in a larger vial containing diethyl ether (4 mL). Light-yellow needle crystals formed within 3 d. Elemental analysis indicates one molecule of water per complex upon atmospheric exposure (22 mg, 29%). IR (ATR): $\tilde{\nu}$ = 3265 (m), 2215 (m), 1639 (s), 1516 (w), 1453 (s), 1389 (s), 1296 (m), 1198 (s), 1179 (s), 1117 (vs), 1036 (w), 861 (w), 836 (s), 764 (s), 726 (s), 716 (s), 632 (w), 597 cm^{-1} (w). $C_{44.25}H_{26}Cl_{0.25}LaN_{14.25}O_{3.75}$ (947.03): calcd. C 55.07, H 2.72, N 20.68; found C 54.62, H 3.12, N 20.37.

Synthesis of $(Et_4N)[Ce(phen)_2(dcnm)_4]$ (6c): $(Et_4N)(dcnm)$ (80 mg, 357 μmol) dissolved in methanol (1 mL) was added to $CeCl_3{\cdot}7H_2O$ (33 mg, 89 μmol) dissolved in methanol (500 μL). 1,10-Phenanthroline monohydrate (35 mg, 177 μmol) dissolved in methanol (2 mL) was added to the reaction solution which was allowed to

slowly evaporate to dryness over a period of one week, yielding clusters of red/orange crystals. The material was removed from the vial and washed with methanol and diethyl ether to yield the final product (7 mg, 8%). IR (ATR): $\tilde{\nu}$ = 3068 (vw), 2994 (vw), 2223 (m), 1592 (vw), 1575 (vw), 1518 (w), 1484 (w), 1424 (m), 1395 (m), 1376 (m), 1258 (m), 1188 (s), 1141 (w), 1099 (vw), 1089 (vw), 1000 (w), 848 (m), 778 (w), 732 (w), 720 cm^{-1} (w). $C_{44}H_{36}CeN_{17}O_4$ (1006.98): calcd. C 52.48, H 3.60, N 23.65; found C 52.16, H 3.59, N 23.67. The initial preparation yielded **6a/b**.

Synthesis of [Ce(phen)$_2$(dcnm)Cl$_2$H$_2$O] (7): 1,10-phenanthroline (47 mg, 237 μmol) and $CeCl_3 \cdot 7H_2O$ (44 mg, 119 μmol) were dissolved in methanol (1 mL). A solution of (Et_4N)(dcnm) (80 mg, 357 μmol) in methanol (1 mL) was added resulting in a light white precipitate. Water (500 μL) was added, causing the precipitate to re-dissolve. The reaction vial was then placed in a larger vial containing diethyl ether (4 mL). Isolated orange block crystals formed within 3 d, insufficient yield for microanalysis. IR (ATR): $\tilde{\nu}$ = 3300 (m), 3251 (m), 3168 (m), 2223 (m), 1668 (s), 1642 (s), 1604 (m), 1590 (m), 1575 (w), 1517 (w), 1484 (w), 1455 (w), 1422 (s), 1188 (m), 1134 (s), 1101 (s), 843 cm^{-1} (m).

Crystallography: Crystals were mounted on fine glass fibres using viscous hydrocarbon oil. Data were collected on Bruker X8 Apex II CCD (**1Pr**, **1Nd**, **1Sm**, **2La**, **2Pr**, **2Nd**, **3La**, **3Sm**, **4La**, **4Ce**, **4Pr**, **4Nd**, **5**, **6a/b**, **6c**, **7**) or Nonius Kappa-CCD (**1La**, **1Ce**, **3Ce**, **3Nd**) diffractometer, both equipped with graphite monochromated Mo-K_α radiation (λ = 0.71073 Å). Data collection temperatures were maintained at 123 K using open-flow N_2 cryostreams. For data collected on the Nonius Kappa-CCD diffractometer integration was carried out by the program DENZO-SMN.[32] For data collected on the Bruker X8 ApexII diffractometer integration was carried out by the program SAINT using the ApexII software suite.[33] All datasets were treated for the effects of absorption. Solutions were obtained by direct methods or Patterson synthesis using SHELXS 97[34] followed by successive refinements using full-matrix least-squares method against F^2 using SHELXL 97.[34] The program X-Seed was used as a graphical SHELX interface.[35] All hydrogen atoms were placed in idealised positions and refined using a riding model to the atom to which they are attached.

CCDC-736604 (for **1La**), -736605 (for **1Ce**), -736606 (for **1Pr**), -736607 (for **1Nd**), -736608 (for **1Sm**), -736609 (for **2La**), -736610 (for **2Pr**), -736611 (for **2Nd**), -736612 (for **3La**), -736613 (for **3Ce**), -736614 (for **3Nd**), -736615 (for **3Sm**), -736616 (for **4La**), -736617 (for **4Ce**), -736618 (for **4Pr**), -736619 (for **4Nd**), -736620 (for **5**), -736621 (for **6a/b**), -736622 (for **6c**), -736623 (for **7**) contain the supplementary crystallographic data for this paper. These data can be obtained free of charge from The Cambridge Crystallographic Data Centre via www.ccdc.cam.ac.uk/data_request/cif.

Crystal Data for 1La: $C_{42}H_{72}LaN_{21}O_{12}$, M = 1202.12, colourless block, 0.23 × 0.19 × 0.15 mm^3, monoclinic, space group $P2_1/n$ (No. 14), a = 12.4968(2), b = 19.3076(4), c = 24.4879(5) Å, β = 95.1870(10)°, V = 5884.3(2) Å^3, Z = 4, D_c = 1.357 g/cm^3, F(000) = 2496, $2\theta_{max}$ = 55.0°, 25406 reflections collected, 13355 unique (R_{int} = 0.0216). Final *GooF* = 1.102, *R1* = 0.0507, *wR2* = 0.1136, R indices based on 12239 reflections with $I > 2\sigma(I)$ (refinement on F^2), 776 parameters, 0 restraints. There are four Et_4N^+ sites per LnL_6^{3-} anion, two of which are over special positions and are refined at 50% occupancy in the ASU.

Crystal Data for 1Ce: $C_{42}H_{72}CeN_{21}O_{12}$, M = 1203.33, purple block, 0.20 × 0.14 × 0.14 mm^3, monoclinic, space group $P2_1/n$ (No. 14), a = 12.4304(2), b = 18.9650(3), c = 24.3960(5) Å, β = 96.4660(10)°, V = 5714.59(17) Å^3, Z = 4, D_c = 1.399 g/cm^3, F(000) = 2500, $2\theta_{max}$ = 55.0°, 36542 reflections collected, 13087 unique (R_{int} = 0.0774). Final *GooF* = 1.031, *R1* = 0.0543, *wR2* = 0.1251, R indices based on 8916 reflections with $I > 2\sigma(I)$ (refinement on F^2), 776 parameters, 0 restraints. There are four Et_4N^+ sites per LnL_6^{3-} anion, two of which are over special positions and are refined at 50% occupancy in the ASU.

Crystal Data for 1Pr: $C_{42}H_{72}N_{21}O_{12}Pr$, M = 1204.12, green block, 0.30 × 0.20 × 0.20 mm^3, monoclinic, space group $P2_1/n$ (No. 14), a = 12.430(3), b = 18.965(4), c = 24.396(5) Å, β = 96.47(3)°, V = 5715(2) Å^3, Z = 4, D_c = 1.400 g/cm^3, F(000) = 2504, $2\theta_{max}$ = 55.0°, 33692 reflections collected, 13108 unique (R_{int} = 0.0275). Final *GooF* = 0.993, *R1* = 0.0414, *wR2* = 0.1075, R indices based on 11668 reflections with $I > 2\sigma(I)$ (refinement on F^2), 776 parameters, 0 restraints. There are four Et_4N^+ sites per LnL_6^{3-} anion, two of which are over special positions and are refined at 50% occupancy in the ASU.

Crystal Data for 1Nd: $C_{42}H_{72}N_{21}NdO_{12}$, M = 1207.45, mauve block, 0.23 × 0.19 × 0.17 mm^3, monoclinic, space group $P2_1/n$ (No. 14), a = 12.3954(3), b = 18.9557(4), c = 24.3969(6) Å, β = 96.2950(10)°, V = 5697.8(2) Å^3, Z = 4, D_c = 1.408 g/cm^3, F(000) = 2508, $2\theta_{max}$ = 55.0°, 39489 reflections collected, 13069 unique (R_{int} = 0.0389). Final *GooF* = 1.008, *R1* = 0.0419, *wR2* = 0.1035, R indices based on 10598 reflections with $I > 2\sigma(I)$ (refinement on F^2), 776 parameters, 0 restraints. There are four Et_4N^+ sites per LnL_6^{3-} anion, two of which are over special positions and are refined at 50% occupancy in the ASU.

Crystal Data for 1Sm: $C_{42}H_{72}N_{21}O_{12}Sm$, M = 1213.56, yellow block, 0.22 × 0.20 × 0.17 mm^3, monoclinic, space group $P2_1/n$ (No. 14), a = 12.3970(3), b = 18.9201(5), c = 24.4292(6) Å, β = 96.0910(10)°, V = 5697.6(2) Å^3, Z = 4, D_c = 1.415 g/cm^3, F(000) = 2516, $2\theta_{max}$ = 55.0°, 40131 reflections collected, 13037 unique (R_{int} = 0.0282). Final *GooF* = 1.041, *R1* = 0.0381, *wR2* = 0.0940, R indices based on 11128 reflections with $I > 2\sigma(I)$ (refinement on F^2), 776 parameters, 0 restraints. There are four Et_4N^+ sites per LnL_6^{3-} anion, two of which are over special positions and are refined at 50% occupancy in the ASU.

Crystal Data for 2La: $C_{31}H_{51}LaN_{21}O_{13.50}$, M = 1074.85, yellow block, 0.26 × 0.20 × 0.17 mm^3, monoclinic, space group $C2/c$ (No. 15), a = 19.5423(5), b = 13.5544(4), c = 37.5927(9) Å, β = 90.6520(10)°, V = 9957.1(5) Å^3, Z = 8, D_c = 1.434 g/cm^3, F(000) = 4408, $2\theta_{max}$ = 55.0°, 26915 reflections collected, 10973 unique (R_{int} = 0.0428). Final *GooF* = 1.238, *R1* = 0.0584, *wR2* = 0.1242, R indices based on 10462 reflections with $I > 2\sigma(I)$ (refinement on F^2), 693 parameters, 0 restraints. One of the cations is disordered over two over-lapping positions whose occupancies were allowed to refine against each other (50:50). There appears to be a sub-stoichiometric amount of water in the lattice which was best modelled as two 25% occupancy molecules with the hydrogen atoms omitted.

Crystal Data for 2Pr: $C_{30.67}H_{50.67}N_{21}O_{12.67}Pr$, M = 1057.17, colourless block, 0.20 × 0.16 × 0.16 mm^3, monoclinic, space group $C2$ (No. 5), a = 19.6073(5), b = 13.4586(3), c = 29.4947(9) Å, β = 108.5450(10)°, V = 7379.1(3) Å^3, Z = 6, D_c = 1.427 g/cm^3, F(000) = 3252, $2\theta_{max}$ = 55.0°, 24701 reflections collected, 15483 unique (R_{int} = 0.0518). Final *GooF* = 1.812, *R1* = 0.0991, *wR2* = 0.2743, R indices based on 14697 reflections with $I > 2\sigma(I)$ (refinement on F^2), 530 parameters, 421 restraints. See **2Nd** for further comments.

Crystal Data for 2Nd: $C_{30.67}H_{50.67}N_{21}NdO_{12.67}$, M = 1060.50, colourless block, 0.20 × 0.16 × 0.16 mm^3, monoclinic, space group $C2$ (No. 5), a = 19.6358(9), b = 13.4574(6), c = 29.5251(14) Å, β = 108.585(1)°, V = 7395.1(6) Å^3, Z = 6, D_c = 1.429 g/cm^3, F(000) = 3258, $2\theta_{max}$ = 55.0°, 21348 reflections collected, 14313 unique (R_{int}

= 0.0560). Final *GooF* = 2.074, *R1* = 0.1059, *wR2* = 0.3013, *R* indices based on 13850 reflections with $I > 2\sigma(I)$ (refinement on F^2), 527 parameters, 421 restraints. The structures of both **2Pr** and **2Nd** were refined as racemic twins, and solutions could not be obtained in *C*2/*c*. The structures were heavily disordered and were therefore refined isotropically (except for **Pr1**, **Pr2** and **Nd2**). Connectivity within the structures is unambiguous in each case and satisfactory *R* factors are obtained. One half of the complete complex in the asymmetric unit is disordered (i.e. six positions for three ligands). The occupancies of these disordered ligands were refined freely and found to be approximately 50:50. Restraints were used on all disordered ligands and on several of the counter-cations. There are modest residual peaks/holes in the vicinity of the rare-earth atoms and some peaks within the sphere of the disordered anionic complex, thought to be signs of further disorder that could not be modelled.

Crystal Data for 3La: $C_{30}H_{36}LaN_{21}O_6$, M = 925.71, yellow block, $0.24 \times 0.21 \times 0.14$ mm^3, trigonal, space group $R\bar{3}$ (No. 148), $a = b$ = 9.9299(3), c = 43.578(2) Å, V = 3721.2(2) Å^3, Z = 3, D_c = 1.239 g/cm^3, $F(000)$ = 1404, $2\theta_{max}$ = 54.9°, 4563 reflections collected, 1815 unique (R_{int} = 0.0193). Final *GooF* = 1.073, *R1* = 0.0363, *wR2* = 0.1035, *R* indices based on 1797 reflections with $I > 2\sigma(I)$ (refinement on F^2), 106 parameters, 7 restraints. μ = 0.917 mm^{-1}. Although there are solvent accessible voids in the structure of 227 Å^3 the voids could not be treated with SQUEEZE due to a significant *R* factor increase. Despite this elemental analysis confirms that only volatile species are enclathrated. A Me_4N^+ cation uses an isotropic model due to heavy disorder. SADI restraints were used for C–N distances in both cations.

Crystal Data for 3Ce: $C_{30}H_{36}CeN_{21}O_6$, M = 926.92, orange block, $0.20 \times 0.19 \times 0.13$ mm^3, trigonal, space group $R\bar{3}$ (No. 148), $a = b$ = 10.0621(14), c = 43.694(9) Å, V = 3831.2(11) Å^3, Z = 3, D_c = 1.205 g/cm^3, $F(000)$ = 1407, Bruker X8 Apex II CCD, Mo-K_α radiation, λ = 0.71073 Å, T = 123(2)K, $2\theta_{max}$ = 55.0°, 8104 reflections collected, 1948 unique (R_{int} = 0.0749). Final *GooF* = 1.111, *R1* = 0.0629, *wR2* = 0.1628, *R* indices based on 1754 reflections with $I > 2\sigma(I)$ (refinement on F^2), 89 parameters, 2 restraints. μ = 0.945 mm^{-1}. See **3La** for extra comments.

Crystal Data for 3Nd: $C_{30}H_{36}N_{21}NdO_6$, M = 931.04, mauve block, $0.24 \times 0.21 \times 0.14$ mm^3, trigonal, space group $R\bar{3}$ (No. 148), $a = b$ = 10.0230(3), c = 43.449(2) Å, V = 3780.2(2) Å^3, Z = 3, D_c = 1.227 g/cm^3, $F(000)$ = 1413, $2\theta_{max}$ = 55.0°, 6092 reflections collected, 1908 unique (R_{int} = 0.0206). Final *GooF* = 1.141, *R1* = 0.0410, *wR2* = 0.1217, *R* indices based on 1904 reflections with $I > 2\sigma(I)$ (refinement on F^2), 89 parameters, 4 restraints. Lp and absorption corrections applied, μ = 1.085 mm^{-1}. See **3La** for extra comments.

Crystal Data for 3Sm: $C_{30}H_{36}N_{21}O_6Sm$, M = 937.15, yellow hexagonal plate, $0.16 \times 0.16 \times 0.12$ mm^3, hexagonal, space group $P6_3/m$ (No. 176), $a = b$ = 9.9838(4), c = 33.483(3) Å, V = 2890.3(3) Å^3, Z = 2, D_c = 1.077 g/cm^3, $F(000)$ = 946, $2\theta_{max}$ = 55.0°, 6886 reflections collected, 2204 unique (R_{int} = 0.0510). Final *GooF* = 1.058, *R1* = 0.0518, *wR2* = 0.1406, *R* indices based on 1604 reflections with $I > 2\sigma(I)$ (refinement on F^2), 85 parameters, 2 restraints. The structure contains void space which was treated with the SQUEEZE routine of PLATON.[36] Only two and a half cations could be located per trianionic complex (with restraints applied to one low occupancy position across a special position). The remaining half cation is presumed to be disordered in the lattice.

Crystal Data for 4La: $C_{21}H_{24}La_1N_9O_9$, M = 685.40, colourless block, $0.25 \times 0.12 \times 0.12$ mm^3, orthorhombic, space group *Pbca* (No. 61), a = 17.8439(7), b = 15.6360(8), c = 20.2224(9) Å, V = 5642.2(4) Å^3, Z = 8, D_c = 1.614 g/cm^3, $F(000)$ = 2736, $2\theta_{max}$ = 50.0°, 26956 reflections collected, 4960 unique (R_{int} = 0.1233). Final *GooF* = 1.091, *R1* = 0.0533, *wR2* = 0.1106, *R* indices based on 3604 reflections with $I > 2\sigma(I)$ (refinement on F^2), 361 parameters, 0 restraints.

Crystal Data for 4Ce: $C_{21}H_{24}Ce_1N_9O_9$, M = 686.61, purple block, $0.20 \times 0.20 \times 0.16$ mm^3, orthorhombic, space group *Pbca* (No. 61), a = 17.8414(7), b = 15.6474(6), c = 20.2029(8) Å, V = 5640.1(4) Å^3, Z = 8, D_c = 1.617 g/cm^3, μ = 1.677 mm^{-1}, $F(000)$ = 2744, $2\theta_{max}$ = 55.0°, 27005 reflections collected, 6402 unique (R_{int} = 0.0271). Final *GooF* = 1.051, *R1* = 0.0268, *wR2* = 0.0619, *R* indices based on 5472 reflections with $I > 2\sigma(I)$ (refinement on F^2), 361 parameters, 0 restraints.

Crystal Data for 4Pr: $C_{21}H_{24}N_9O_9Pr_1$, M = 687.40, green block, $0.20 \times 0.18 \times 0.18$ mm^3, orthorhombic, space group *Pbca* (No. 61), a = 17.8447(3), b = 15.6260(2), c = 20.1784(3) Å, V = 5626.57(15) Å^3, Z = 8, D_c = 1.623 g/cm^3, $F(000)$ = 2752, $2\theta_{max}$ = 55.0°, 20875 reflections collected, 6324 unique (R_{int} = 0.0202). Final *GooF* = 1.069, *R1* = 0.0248, *wR2* = 0.0495, *R* indices based on 5571 reflections with $I > 2\sigma(I)$ (refinement on F^2), 361 parameters, 0 restraints.

Crystal Data for 4Nd: $C_{21}H_{24}N_9Nd_1O_9$, M = 690.73, colourless block, $0.25 \times 0.25 \times 0.20$ mm^3, triclinic, space group $P\bar{1}$ (No. 2), a = 7.8856(2), b = 9.9484(3), c = 17.5475(5) Å, α = 91.457(2), β = 90.081(2), γ = 98.281(2)°, V = 1361.77(7) Å^3, Z = 2, D_c = 1.685 g/cm^3, μ = 1.972 mm^{-1}, $F(000)$ = 690, $2\theta_{max}$ = 55.0°, 17485 reflections collected, 6221 unique (R_{int} = 0.0308). Final *GooF* = 1.084, *R1* = 0.0228, *wR2* = 0.0455, *R* indices based on 5829 reflections with $I > 2\sigma(I)$ (refinement on F^2), 361 parameters, 0 restraints.

Crystal Data for 5: $C_{44.25}H_{24}Cl_{0.25}LaN_{14.25}O_{2.75}$, M = 947.05, colourless block, $0.23 \times 0.20 \times 0.14$ mm^3, monoclinic, space group $P2_1/c$ (No. 14), a = 10.6849(2), b = 17.8544(4), c = 21.2592(4) Å, β = 99.2490(10)°, V = 4002.94(14) Å^3, Z = 4, D_c = 1.571 g/cm^3, μ = 1.145 mm^{-1}, $F(000)$ = 1890, $2\theta_{max}$ = 55.0°, 44449 reflections collected, 9159 unique (R_{int} = 0.0385). Final *GooF* = 1.463, *R1* = 0.0736, *wR2* = 0.1352, *R* indices based on 8716 reflections with $I > 2\sigma(I)$ (refinement on F^2), 587 parameters, 8 restraints. Disordered dcnm ligand and chloride were refined at 75:25 occupancy, respectively. ISOR restraint used on the chloride and DFIX command used to restrain the portion of the dcnm ligand near the chloride partial occupancy.

Crystal Data for 6a/b: $C_{44}H_{36}Ce_1N_{17}O_4$, M = 1007.02, purple needle, $0.30 \times 0.30 \times 0.05$ mm^3, monoclinic, space group *C*2/*c* (No. 15), a = 40.4476(10), b = 20.2788(5), c = 17.9729(4) Å, β = 111.593(1)°, V = 13707.3(6) Å^3, Z = 12, D_c = 1.464 g/cm^3, μ = 1.059 mm^{-1}, $F(000)$ = 6108, $2\theta_{max}$ = 50.0°, 16531 reflections collected, 9928 unique (R_{int} = 0.0800). Final *GooF* = 1.200, *R1* = 0.1034, *wR2* = 0.2110, *R* indices based on 7467 reflections with $I > 2\sigma(I)$ (refinement on F^2), 899 parameters, 6 restraints.

Crystal Data for 6c: $C_{44}H_{36}CeN_{17}O_4$, M = 1007.02, red block, $0.30 \times 0.20 \times 0.20$ mm^3, triclinic, space group $P\bar{1}$ (No. 2), a = 10.6370(8), b = 13.0550(9), c = 16.6799(13) Å, α = 82.771(2), β = 84.624(2), γ = 82.837(2)°, V = 2272.8(3) Å^3, Z = 2, D_c = 1.472 g/cm^3, $F(000)$ = 1018, $2\theta_{max}$ = 55.0°, 19958 reflections collected, 10291 unique (R_{int} = 0.0212). Final *GooF* = 1.047, *R1* = 0.0551, *wR2* = 0.1366, *R* indices based on 9546 reflections with $I > 2\sigma(I)$ (refinement on F^2), 647 parameters, 0 restraints. Lp and absorption corrections applied, μ = 1.064 mm^{-1}. The site occupancies of two disordered dcnm ligands were refined freely and both found to be 47:53. The Et_4N^+ counter cation is refined isotropically due to extensive disorder which could not be satisfactorily modelled.

Crystal Data for 7: $C_{27}H_{18}Ce_1Cl_2N_7O_2$, M = 683.50, purple block, $0.30 \times 0.12 \times 0.12$ mm^3, triclinic, space group $P\bar{1}$ (No. 2), a = 7.0442(14), b = 10.308(2), c = 19.209(4) Å, α = 98.66(3), β = 90.23(3), γ = 109.45(3)°, V = 1298.0(4) Å^3, Z = 2, D_c = 1.749 g/cm^3, μ = 2.000 mm^{-1}, $F(000)$ = 674, $2\theta_{max}$ = 55.0°, 13931 reflections collected, 5958 unique (R_{int} = 0.0198). Final *GooF* = 1.053, *R1* = 0.0199, *wR2* = 0.0477, *R* indices based on 5655 reflections with $I > 2\sigma(I)$ (refinement on F^2), 360 parameters, 0 restraints.

Supporting Information (see also the footnote on the first page of this article): Supplementary figures and tables of hydrogen bonding parameters.

Acknowledgments

We thank the Australian Research Council for funding and for an Australian Post-Doctoral fellowship (D. R. T.). A. S. R. C. is grateful for an Australian Postgraduate Award scholarship.

[1] a) D. R. Turner, S. R. Batten, *Coordination Chemistry of Small, Dicyanomethanide-Based Ligands*, in: *Coordination Chemistry Research Trends* (Eds.: T. W. Cartere, K. S. Verley), **2008**; b) A. M. Golub, H. Köhler, V. V. Skopenko, *Chemistry of Pseudohalides*, in: *Topics in Inorganic and General Chemistry, Monograph 21* (Ed.: R. J. Clark), Elsevier, Amsterdam, **1986**; c) G. Longo, *Gazz. Chim. Ital.* **1931**, *61*, 575–583; d) G. G. Sadikov, Y. L. Zub, V. V. Skopenko, V. P. Nikolaev, M. A. Porai-Koshits, *Koord. Khim.* **1984**, *10*, 1253–1262; e) Y. L. Zub, G. G. Sadikov, V. V. Skopenko, M. A. Porai-Koshits, V. P. Nikolaev, *Koord. Khim.* **1985**, *11*, 532–539; f) D. S. Bohle, B. J. Conklin, C.-H. Hung, *Inorg. Chem.* **1995**, *34*, 2569–2581; g) N. Arulsamy, D. S. Bohle, B. G. Doletski, *Inorg. Chem.* **1999**, *38*, 2709–2715; h) V. Jacob, S. Mann, G. Huttner, O. Walter, L. Zsolnai, E. Kaifer, P. Rutsch, P. Kircher, E. Bill, *Eur. J. Inorg. Chem.* **2001**, 2625–2640.

[2] M. Hvastijová, J. Kohout, J. W. Buchler, R. Boča, J. Kožíšek, L. Jäger, *Coord. Chem. Rev.* **1998**, *175*, 17–42.

[3] a) D. J. Price, S. R. Batten, K. J. Berry, B. Moubaraki, K. S. Murray, *Polyhedron* **2003**, *22*, 165–176; b) A. S. R. Chesman, D. R. Turner, B. Moubaraki, K. S. Murray, G. B. Deacon, S. R. Batten, *Chem. Commun.* **2007**, 3541–3543; c) M. Hvastijová, J. Kohout, J. Kožíšek, I. Svoboda, *J. Coord. Chem.* **1999**, *47*, 573–579; d) J. W. Buchler, M. Hvastijová, J. Kohout, J. Kožíšek, *Transition Met. Chem.* **1998**, *23*, 215–220; e) M. Hvastijová, J. Kožíšek, J. Kohout, J. G. Díaz, *Inorg. Chim. Acta* **1995**, *236*, 163–165; f) A. S. R. Chesman, D. R. Turner, G. B. Deacon, S. R. Batten, *Chem. Asian J.* **2009**, *4*, 761–769; g) A. S. R. Chesman, D. R. Turner, B. Moubaraki, K. S. Murray, G. B. Deacon, S. R. Batten, *Eur. J. Inorg. Chem.* **2010**, 59–73.

[4] N. Arulsamy, D. Bohle, *J. Org. Chem.* **2000**, *65*, 1139–1143.

[5] a) S. A. Cotton, in: *Comprehensive Coordination Chemistry II* (Eds.: J. A. McCleverty, T. J. Meyer), **2004**, vol. 3, pp. 93–188; b) F. A. Cotton, G. Wilkinson, *Advanced Inorganic Chemistry*, 5th ed., John Wiley & Sons, New York, **1988**.

[6] a) J.-C. G. Bünzli, *Acc. Chem. Res.* **2006**, *39*, 53–61; b) G. Meyer, *J. Alloys Compd.* **2000**, *300–301*, 113–122.

[7] a) J. Paulovi, F. Cimpoesu, M. Ferbinteanu, K. Hirao, *J. Am. Chem. Soc.* **2004**, *126*, 3321–3323; b) J.-P. Costes, F. Dahan, A. Dupuis, J.-P. Laurent, *Chem. Eur. J.* **1998**, *4*, 1616–1620; c) J.-P. Costes, J. M. Clemente-Juan, F. Dahan, F. Nicodème, M. Verelst, *Angew. Chem. Int. Ed.* **2002**, *41*, 323–325.

[8] a) B. H. Bakker, M. Goes, N. Hoebe, H. J. van Ramesdonk, J. W. Verhoeven, M. H. V. Werts, J. W. Hofstraat, *Coord. Chem. Rev.* **2000**, *208*, 3–16; b) M. D. Ward, *Coord. Chem. Rev.* **2007**, *251*, 1663–1677; c) N. Sabbatini, M. Guardigli, J.-M. Lehn, *Coord. Chem. Rev.* **1993**, *123*, 201–228.

[9] a) G. B. Deacon, P. MacKinnon, R. S. Dickson, G. N. Pain, B. O. West, *Appl. Organomet. Chem.* **1990**, *4*, 439–449; b) M. Seitz, A. G. Oliver, K. N. Raymond, *J. Am. Chem. Soc.* **2007**, *129*, 11153–11160.

[10] a) F. Nicolò, J.-C. G. Bünzli, G. Chapuis, *Acta Crystallogr., Sect. C* **1988**, *44*, 1733–1738; b) A. S. R. Chesman, D. R. Turner, G. B. Deacon, S. R. Batten, *Acta Crystallogr., Sect. E* **2006**, *62*, m1942–m1943; c) W.-J. Lu, L.-P. Zhang, H.-S. Chan, T.-L. Chan, T. C. W. Mak, *Polyhedron* **2004**, *23*, 1089–1096; d) X. Li, W. Liu, Z. Guo, M. Tan, *Inorg. Chem.* **2003**, *42*, 8735–8738; e) L. Jianmin, Z. Huaqianga, Z. Yugen, C. Jinhua, K. Yanxiong, W. Quanming, W. Xintao, *Cryst. Res. Technol.* **1999**, *34*, 925–928.

[11] A. Clearfield, R. Gopal, R. W. Olsen, *Inorg. Chem.* **1977**, *16*, 911–915.

[12] X. Chen, S. Lim, C. E. Plecnik, S. Liu, B. Du, E. A. Meyers, S. G. Shore, *Inorg. Chem.* **2005**, *44*, 6052–6061.

[13] R. Schwesinger, K. Piontek, W. Littke, H. Prinzbach, *Angew. Chem.* **1985**, *97*, 344–345; *Angew. Chem. Int. Ed. Engl.* **1985**, *24*, 318–319.

[14] G. M. Davies, R. J. Aarons, G. R. Motson, J. C. Jeffery, H. Adams, S. Faulkner, M. D. Ward, *Dalton Trans.* **2004**, 1136–1144.

[15] B. S. Hammes, X. Luo, B. S. Chohan, M. W. Carrano, C. J. Carrano, *J. Chem. Soc., Dalton Trans.* **2002**, 3374–3380.

[16] A. S. R. Chesman, D. R. Turner, E. I. Izgorodina, G. B. Deacon, S. R. Batten, *Dalton Trans.* **2007**, *60*, 1371–1373.

[17] W. J. Evans, J. M. Perotti, R. J. Doedens, J. W. Ziller, *Chem. Commun.* **2001**, 2326–2327.

[18] a) Z. Wu, X. Zhou, W. Zhang, Z. Xu, X. You, X. Huang, *J. Chem. Soc., Chem. Commun.* **1994**, 813–814; b) A. Venugopal, A. Willner, A. Heppa, N. W. Mitzel, *Dalton Trans.* **2007**, 3124–3126; c) A. Venugopal, A. Hepp, T. Pape, A. Mix, N. W. Mitzel, *Dalton Trans.* **2008**, 6628–6633.

[19] a) D. R. Turner, S. N. Pek, S. R. Batten, *Chem. Asian J.* **2007**, *2*, 1534–1539; b) D. R. Turner, S. R. Batten, *CrystEngComm* **2008**, *10*, 170–172; c) D. R. Turner, S. N. Pek, S. R. Batten, *New J. Chem.* **2008**, *32*, 719–726; d) D. R. Turner, S. N. Pek, S. R. Batten, *CrystEngComm* **2009**, *11*, 87–93; e) D. R. Turner, S. N. Pek, J. D. Cashion, B. Moubaraki, K. S. Murray, S. R. Batten, *J. Chem. Soc., Dalton Trans.* **2000**, *48*, 6877–6879; f) D. R. Turner, R. MacDonald, W. T. Lee, S. R. Batten, *CrystEngComm* **2009**, *11*, 298–305.

[20] D. R. Turner, M. Henry, C. Wilkinson, G. J. McIntyre, S. A. Mason, A. E. Goeta, J. W. Steed, *J. Am. Chem. Soc.* **2005**, *127*, 11063–11074.

[21] Using graph set nomenclature, see J. Bernstein, R. E. Davis, L. Shimoni, N.-L. Chang, *Angew. Chem. Int. Ed. Engl.* **1995**, *34*, 1555–1573.

[22] A. S. R. Chesman, D. R. Turner, G. B. Deacon, S. R. Batten, *J. Coord. Chem.* **2007**, *60*, 2191–2196.

[23] a) J. D. J. Backer-Dirks, J. E. Cooke, A. M. R. Galas, J. S. Ghotra, C. J. Gray, F. A. Hart, M. B. Hursthouse, *J. Chem. Soc., Dalton Trans.* **1980**, 2191–2198; b) Y. Jingwen, L. Baosheng, W. Jingqin, Z. Shaohui, *Chem. J. Chin. Univ.* **1987**, 559; c) R. D. Rogers, A. N. Rollins, *J. Chem. Crystallogr.* **1994**, *24*, 321–329; d) J.-C. G. Bünzli, B. Klein, D. Wessner, *Inorg. Chim. Acta* **1980**, *44*, L147–L149.

[24] a) J.-C. G. Bünzli, B. Klein, D. Wessner, *Inorg. Chim. Acta* **1981**, *54*, L43–L46; b) F. Yuguo, Y. Jingshen, L. Pinzhe, J. Zhongshen, Y. Fenglan, Z. Shugong, N. Jiazuan, *Chin. J. Appl. Chem.* **1986**, *3*, 35; c) F. Nicolò, J.-C. G. Bünzli, G. Chapuis, *Acta Crystallogr., Sect. C* **1988**, *44*, 1733–1738.

[25] C. A. Hunter, K. R. Lawson, J. Perkins, C. J. Urch, *J. Chem. Soc., Perkin Trans. 2* **2001**, 651–669.

[26] a) F. H. Allen, *Acta Crystallogr., Sect. B* **2002**, *58*, 380–388; b) Cambridge Structural Database, v. 5.31, November **2009**.

[27] S. A. Cotton, V. Franckevicius, R. E. Howa, B. Ahrens, L. L. Ooi, M. F. Mahon, P. R. Raithby, S. J. Teat, *Polyhedron* **2003**, *22*, 1489–1497.

[28] a) M. Fréchette, I. R. Butler, R. Hynes, C. Detellier, *Inorg. Chem.* **1992**, *31*, 1650–1656; b) Q.-Y. Lin, Y.-L. Feng, *Z. Kristallogr. - New Cryst. Struct.* **2003**, *218*, 531–532; c) Y.-Q. Zheng, L.-X. Zhou, J.-L. Lin, S.-W. Zhang, *Z. Anorg. Allg. Chem.* **2001**, *627*, 1643–1646; d) V. B. Rybakov, V. N. Zakharov, A. L. Kamyshbyi, L. A. Aslanov, A. P. Suisalu, *Koord. Khim.* **1991**, *17*, 1061–1064; e) D.-Y. Wei, J.-L. Lin, Y.-Q. Zheng, *J. Coord. Chem.* **2002**, *55*, 1259–1262; f) G. G. Sadikov, A. S. Antsyshkina, I. A. Kuznetsova, M. N. Rodnikova, *Crystallogr. Rep.* **2006**, *51*, 47–52; g) G. G. Sadikov, A. S. Antsyshkina, I. A. Kuznetsova, M. N. Rodnikova, *Crystallogr. Rep.* **2006**, *51*, 271–277; h) D. L. Kepert, I. L. Semenova, A. N. Sobolev, A. H. White, *Aust. J. Chem.* **1996**, *49*, 1005–1008.

[29] For examples of geometric isomers in lanthanoid coordination chemistry see: a) V. Chebolu, R. R. Whittle, A. Sen, *Inorg. Chem.* **1985**, *24*, 3082–3085; b) A. Sen, V. Chebolu, A. L. Rheingold, *Inorg. Chem.* **1987**, *26*, 1821–1823; c) S. Beaini, G. B. Deacon, E. E. Delbridge, P. C. Junk, B. W. Skelton, A. H. White, *Eur. J. Inorg. Chem.* **2008**, 4586–4596; d) S. Beaini, G. B. Deacon, M. Hilder, P. C. Junk, D. R. Turner, *Eur. J. Inorg. Chem.* **2006**, 3434–3441.

[30] For examples of M–Cl as hydrogen-bond acceptors see: a) L. Brammer, *Dalton Trans.* **2003**, 3145–3157; b) D. R. Turner, B. Smith, A. E. Goeta, I. Radosavljevic-Evans, D. A. Tocher, J. A. K. Howard, J. W. Steed, *CrystEngComm* **2004**, *6*, 633–641.

[31] A. S. R. Chesman, D. R. Turner, B. Moubaraki, K. S. Murray, G. B. Deacon, S. R. Batten, *Chem. Eur. J.* **2009**, *15*, 5203–5207.

[32] Z. Otwinowski; Minor, W. in *Methods in Enzymology*, vol 276. (Eds.: C. W. Carter Jr., R. M. Sweet), Academic Press, New York, **1997**, p. 307.

[33] *Apex2*, v2.0, Bruker AXS Ltd., Madison, WI, USA, **2005**.

[34] G. M. Sheldrick, *Acta Crystallogr., Sect. A* **2008**, *64*, 112–122.

[35] L. J. Barbour, *J. Supramol. Chem.* **2001**, *1*, 189–191.

[36] H. D. Flack, *Acta Crystallogr., Sect. A* **1983**, *39*, 876–881.

[37] A. L. Spek, *J. Appl. Crystallogr.* **2003**, *36*, 7–13.

Received: March 6, 2010
Published Online: May 19, 2010

